Performance and Characterization of Bimetallic Joints through Conventional and Non-Conventional Welding Processes

A dissertation submitted in partial fulfilment of requirement for the degree of

Master of Engineering

in

Production Engineering

Submitted by

Sapna Kumari

801785011

Under the guidance of

Dr. Deepa Mudgal
Assistant Professor

Dr. Dheeraj Gupta
Associate Professor

THAPAR INSTITUTE
OF ENGINEERING & TECHNOLOGY
(Deemed to be University)

Department of Mechanical Engineering
Thapar Institute of Engineering & Technology
(Deemed to be University)
Patiala-147004, India

July 2019

Certificate

I hereby declare that the work done in this dissertation entitled **Performance and characterization of bimetallic joints through conventional and non-conventional welding processes** submitted towards partial fulfilment of requirement for award of degree **of Master** of **Engineering** in **Production Engineering, Thapar Institute of Engineering and Technology, Patiala,** is an authentic record of the work carried out by me under the supervision of **Dr. Deepa Mudgal, Assistant Professor, Mechanical Engineering Department , Thapar Institute of Engineering and Technology** and **Dr. Dheeraj Gupta, Associate Professor, Mechanical Engineering Department , Thapar Institute of Engineering and Technology.** The matter embodied in this report has not been submitted in part or full to any other university or institute for the award of any degree.

Dated: 22/08/19

Sapna Kumari

801785011

This is to certify that above declaration made by the student concerned is correct to the best of our knowledge and belief.

Deep S 22/08/19

Dr. Deepa Mudgal

Assistant Professor
Mechanical Engineering Department
Thapar Institute of Engineering and
Technology , Patiala-147004

22/08/19

Dr. Dheeraj Gupta

Associate Professor
Mechanical Engineering Department
Thapar Institute of Engineering and
Technology, Patiala -147004

Acknowledgments

I would like to express my profound gratitude and a very sincere thanks to **Dr. Deepa Mudgal (Assistant Professor) and Dr. Dheeraj Gupta (Associate Professor), Mechanical Engineering Department, Thapar Institute of engineering and technology, Patiala** for their commendable and praiseworthy guidance, boost up and inspirations which helped me to complete the work.

I am also very thankful to **Dr. T.P Singh,** Head of Department**, Mechanical Engineering Department, Thapar Institute of engineering and technology, Patiala** who has done his best to lead us to the goal and encouraged us to keep our progress on track.

I am happy to oblige to faculty and staff members of the Mechanical Engineering Department for their continuous help and efforts. I am also very grateful to **Mr. Sarabjeet Singh, Sandeep Bansal (PhD scholar), Mechanical Engineering Department** for his valuable help and efforts for my project.

I would end up with, expressing my deepest gratitude to my family for their unstoppable encouragement and blessing which boosted me to the work on time with full enthusiasm.

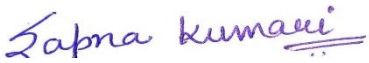

Sapna Kumari

801785011

Abstract

The purpose of this work is to study the performance of bimetallic joint processed through conventional (TIG welding) and non -conventional technique (microwave energy). The hot corrosion behaviour of the samples was also studied in simulated (40% Na_2SO_4-40% K_2SO_4-1O%Nacl-10%KCl) as well as in the actual environment of the boiler. Characterization of joints was done by XRD, SEM-EDS. Tensile testing and Vickers micro hardness were carried out. Tensile strength and micro hardness value of the microwave processed sample have a higher value as compared to the TIG welded sample. In a simulated environment of the boiler, 25 cycles were performed in a laboratory furnace at a temperature of 750℃. Each cycle is of 1 h 20 min in which 1 h is of heating duration and 20 min is of cooling at room temperature. Weight of the samples was noted down after each cycle. Study of hot corrosion in the actual environment is performed in a husk fired boiler power plant working at Nectar Pvt.Ltd., Dera bassi, Chandigarh. XRD, SEM-EDS and X-Ray mapping were used to characterize the product of corrosion. The results show that microwave welded joints performed better in both simulated and actual boiler environment. Although the surface oxide formed on both the cases were porous. However, XRD analysis revealed the formation of sulphides, which cause the sulphidation reaction leading to catastrophic failure of weld joints of the TIG welded samples.

Table of Contents

Lists of Figures

LIST OF TABLES

Abbreviations

ASTM	American Society for Testing and Materials.
EDS	Energy Dispersive X-Ray Spectroscopy.
EM	Electromagnetic Spectrum.
EPMA	Electron Probe Micro Analyzer.
HAZ	Heat Affected Zone.
MHH	Microwave Hybrid Heating.
MW	Microwave.
SEM	Scanning Electron Microscopy.
TIG	Tungsten Inert Gas.
UTS	Ultimate tensile strength.
K_p	Parabolic rate constant
VHN	Vickers hardness number
Wt.%	Weight %
mpy	Mils per year

Chapter 1

Introduction

1.1 Corrosion Problem Occurring at the Weld Joint of Boiler

Every year, there is an economic loss due to the failure of components of boiler. High temperature corrosion, creep are the most prominent causes for the failures of the boiler. Due to the corrosion problems, industries are experiencing sudden breakdown and shutdown. Such failures are crucial reason for the unscheduled maintenance disruptions. Because of the exhaustion of the fuel, biomass-based fuels like husk, straw is in use widely. In these fuels, there is the presence of sulfur, vanadium, and sodium as contaminants. During the combustion process Na,S form a compound Na_2SO_4 and vanadium forms V_2O_5. The deposits of the $Na_2SO_4$and V_2O_5 is seen on the many components in the service which involves the high temperature were in touch with gases with lots of impurities like Na, S [1**].** This arises in serious corrosion attack by high-temperature corrosion, chlorination, sulfidation, and oxidation [2]. The presence of corrosive build-up layer on the surface of the component causes hot corrosion which adversely affects the service life of components [3]**.** A failure of the boiler is mostly because of the failures of the weld joint due to corrosion. The failure of the joint of austenite stainless and ferrite steel in the steam plants is a serious issue [4].The performance of gas tungsten arc weldments of stainless steel and Monel 400 in the environment of molten salts of K_2SO_4-NaCl at a temperature of 600°C has been reported by Devendernath et.al [5], that weld joints fails at high temperature. Premature failure of weld joint occurs at intermediate temperature. Even after the welding done by advanced techniques, the issue of carbide development isn't yet totally eliminated for the joints when they are presented to cyclic high-temperature working conditions.

1.2 Joining Process Used in Boiler

A boiler, enclosed vessel which uses, coal, oil and gas as a fuel to generate power. Boiler experiences different types of environment either oxidizing conditions, reducing conditions and high temperature etc. To sustain that environment, selection of construction materials and welding techniques are the two most important factors to be concerned about. Dissimilar

welding is widely used in an application which involves high temperature conditions. Welding two dissimilar metals is difficult as compared to the welding of similar metals because the two metals differ in mechanical properties, chemical and thermal properties. The most common welding technique which is being in use since long is TIG welding in most of the industries. However the speed of welding is slow with respect to metal inert gas welding, but still, former poses superior qualities. Precise and perfect weld can be achieved with suitable filler metals, by the TIG welding. Through TIG welding various metals can be weld such as stainless steel, copper, aluminum, mild steel. Corrosion resistance of weldments of TIG welding is superior to that of shielded metal arc welding [6]. Due to high welding speed, above 0.7 m/ min cause hot cracking. Hot cracking is the main reason for the damaging of weld joint of 7CrMoVTiB, produced by submerged arc welding [7]. Electron beam weldments have higher tensile strength, impact strength and compressive strength as compared to the friction weldments [8]. However the weldments produced by electron beam welding technique is more susceptible to the corrosion than parent metal when subjected to an environment of molten salts of (Na_2SO_4 – 60%V_2O_5, K_2SO_4- 60% NaCl. Sputtering and spalling of the oxides observed [9]. Failure of the weld joint, produced through the friction stir welding when subjected to a simulated environment of biomass fed boiler, occurred. The weld joints experienced an extreme corrosion as the oxides formed were not protective [10].The performance of gas tungsten arc weldments of stainless steel and Monel 400 in the environment of molten salts of K_2SO_4-NaCl at a temperature of 600°C has been reported [11]. It was clearly reported, that weld joints fails at high temperature. Premature failure of weld joint occurs at intermediate temperature. HAZ zone has high hardness along with microstructural instability, responsible for the failure due crack generation [12]. HAZ does not have good corrosion behaviour and good mechanical properties, causes the failure of weld. To extend the lifetime of welded boiler, corrosion behavior and mechanical properties of HAZ has to improve [13]. A study has been reported and showed the higher temperature behavior dissimilar weldments of austenitic stainless steel (AISI 316L) and medium carbon steel (AISI 1045), produced by frictional welding. It was observed that weld joints have more hardness value than the parent metals and resulted in failure in high temperature services [14]. In dissimilar, welding due to metallurgical incompatibility, cause HAZ cracking or might produces such microstructure of the weld metal which cannot offer satisfactory corrosion and mechanical performance [15]. Even the presence of small defect or

pre-exiting crack can cause catastrophic failure. As they grow with the course of time and leads to catastrophic failure of individual part, heat exchanger and boiler [16]. It is reported that, coal based boiler have experienced problems of carburization in reheaters [17]. Despite the fact that the most well-known welding techniques are MIG, plasma and TIG, because of the high temperatures during the welding, causes the formation of precipitates in HAZ. This adversely affected the mechanical properties [18]. Laser arc welding is not being accepted widely due the two main barriers, high cost of installment and to understand the relation between the properties of material and the welding condition, lots of research needs to finish although it can produce good weld joints [19]. Even after the employing the advanced technique for welding, the problem of carbide problem is not eliminated completely, all starts due to the heat affected zone which makes the weld joints more prone to failure. So as an alternative solution for the above mentioned problem, microwave energy is being employed for joining the materials, mainly steels and better properties are reported in the literature. The produced joint is HAZ free and crack free [20].The joints produced through microwave processing have better metallurgical bonding. Tensile strength of the joint also improved as proper fusion between the powder slurry and materials takes place [21]. It was also reported that clad developed through microwave energy has good resistance to crack formation because of the availability of Ni based matrix having ductile behaviour [22]. Introduction of microwave energy is discussed in detail further in the subsequent section.

1.3 Introduction to Microwaves

Microwave is one of the regions of the electromagnetic spectrum (EM) in which magnetic and electrical waves propagate perpendicular to each other with wavelength and frequency ranges 30 cm to1mm and 300MHz to 300 GHz respectively, shown in Figure 1.1 [23]. This frequency range permitted the use of microwaves in many applications, like heating purpose in industrial, system of communication, materials processing, processing of food, medical applications, etc. [24]. The frequency commonly used for domestic microwaves in India is 2.45 GHz and with the purpose of heating the food. These ovens are designed for material processing applications that are used inmany industrial applications [25-26].

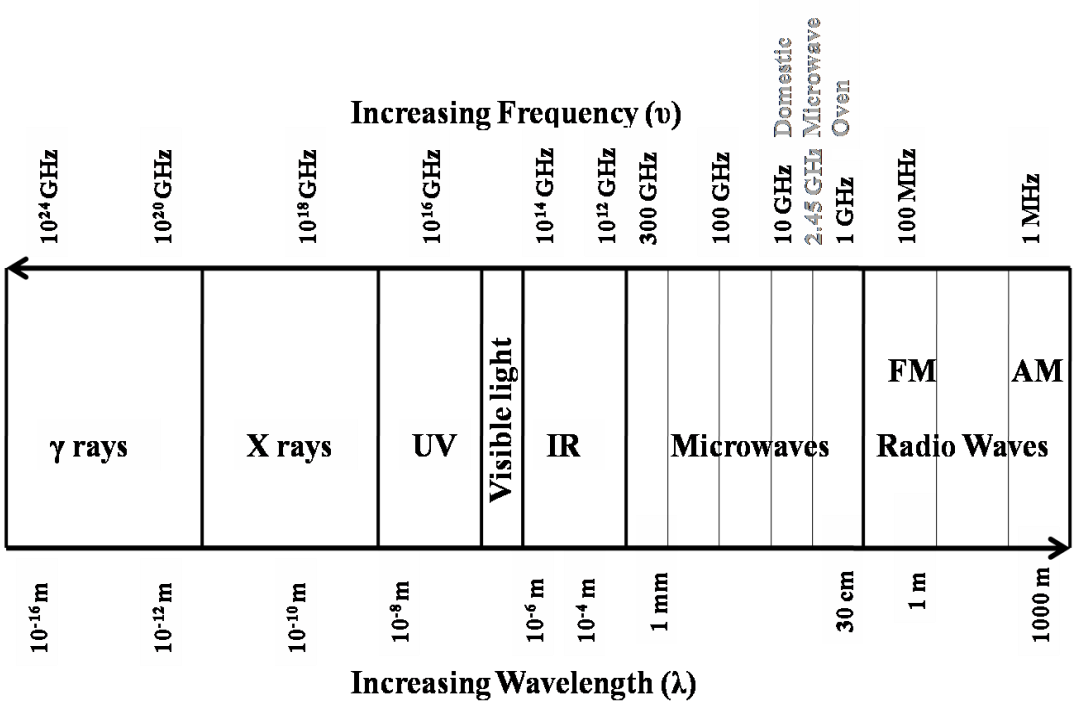

Figure1.1 Electromagnetic Spectrum of the microwave band [23].

The main applications of microwaves have been in communication systems such as radar, satellite communications, and television broadcasts. The heating effect of microwaves was discovered by chance by Spencer, and in 1945 the first patent [27] of the microwave oven was filed for heating. Over time, microwave ovens become one of the most popular household items for heating food, due to the properties of higher heating rates, lower energy consumption and shorter processing times. These beneficial and unique properties of microwaves have caught the attentions of many researchers to process various materials using microwave heating phenomena. The use of microwaves to heat materials has been further explored by researchers in the field of material processing to get the benefit of higher heating rates with shorter processing times [28-30]. These studies have led to the use of microwaves in chemical reactions, processing of ceramic and metal materials, steelmaking, alternative energy recovery sources, etc. [31]. Microwaves have been shown to be useful for treating various types of materials having a high rate of heating and eco-friendly properties.

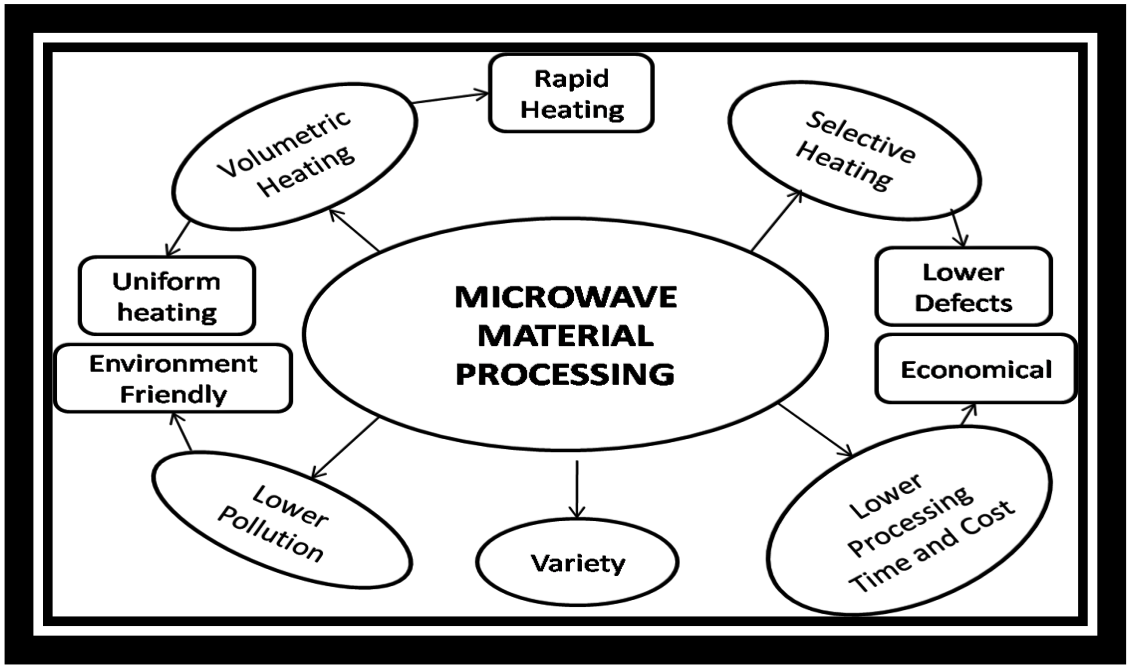

Figure1.2 Characteristics of microwave materials processing.

Microwaves absorption at the atomic level of material under processing resulted in the volumetric heating of the selected materials. Due to volumetric heating, the gradient of thermal is less and as well as the heating rate is also fast. Microwave joining in contrast to the conventional s consumes less energy and time of processing is also less, because of the microwave's volumetric heating characteristics [32-34]. One more advantage of microwave processing is the absence of HAZ zone along with fewer defects as compared to the conventional heating and this happens by exposing the materials to the selective heating. Application of the microwave energy is also applied for processing of ceramic and achieved success with enhanced properties, reported by many authors [35-36].

1.3.1 Theory of Microwave Heating

Heating of the material occurs by direct absorption of microwaves in the entire volume ofthe material. However, the physical property of the material has a critical role in the effective and productive heating of material by microwave radiation. Interaction of materials with the microwaves is different from material to material that is shown in Figure 1.3, and classifies the three major groups of materials [37].

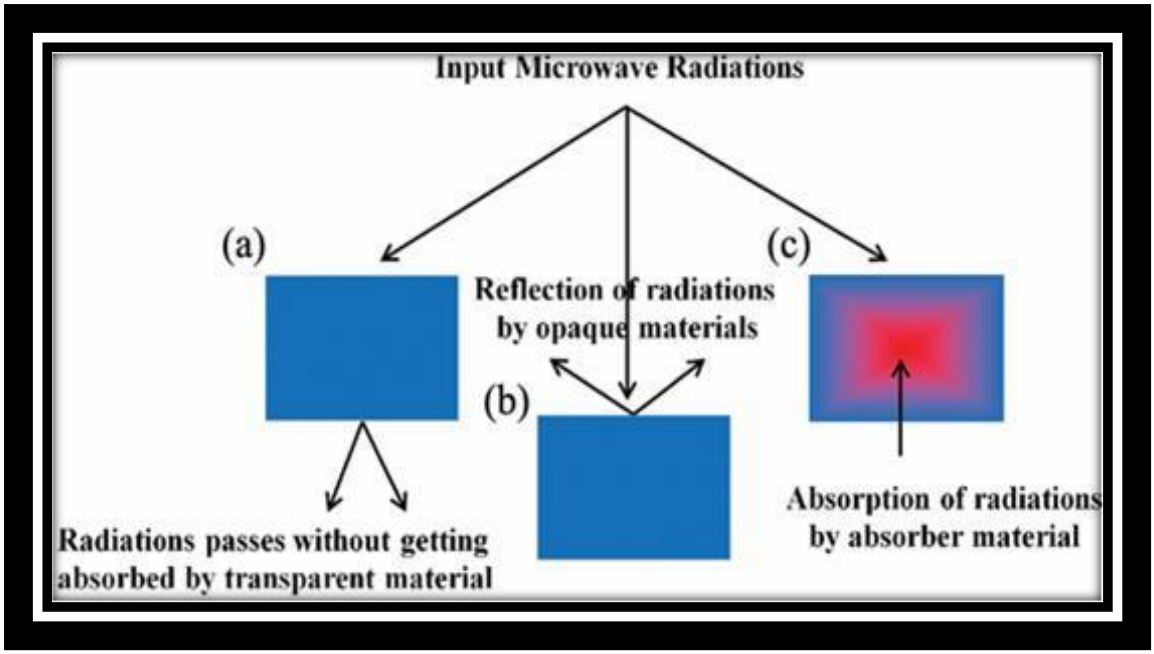

Figure1.3. Interaction of microwaves with different types of materials [37]

Since transparent materials like glass do not absorb microwaves and pass easily without losses, there is no heating. Bulk materials, on the other hand, cannot pass or absorb microwaves, but cause surface reflections. This forms plasma and heats the surface of the body. However, the third category of materials, mainly known as microwave coupling materials (dielectric materials), absorb microwaves easily and convert these radiations into heat.

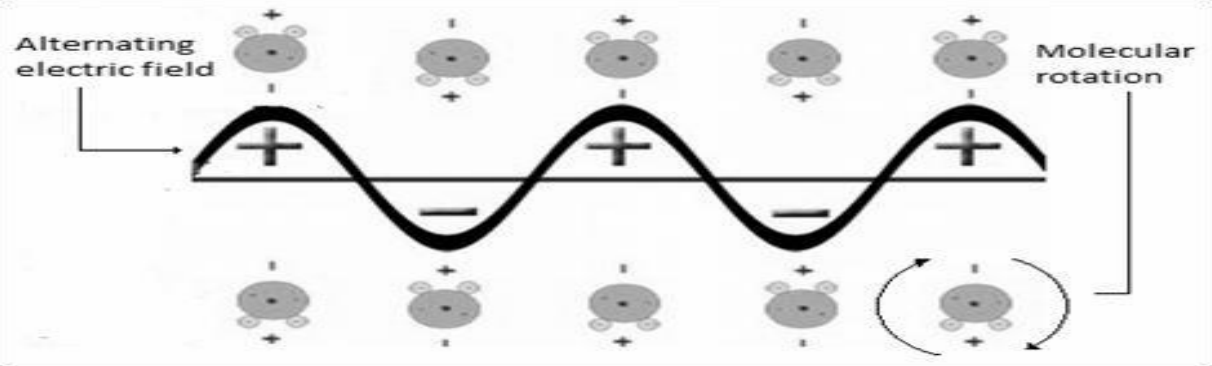

Figure1.4. Mechanism of dipole rotation subjected to microwaves

This exothermic is a complex phenomenon caused primarily by the mechanism of dipolar loss or reorientation. When the material is exposed to microwaves, the electric and magnetic

fields alternate 2.45 billion times per second which cause rotation of dipoles as shown in Figure.1.4.

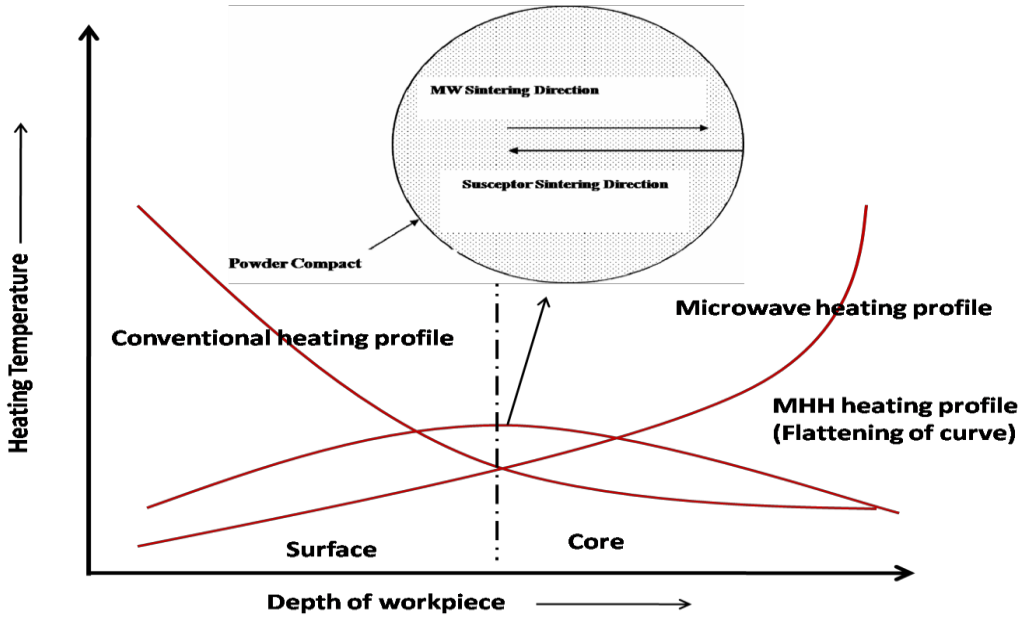

Figure. 1. 5.Heating profile for conventional, microwave and microwave hybrid heating of materials

To employ the application of microwaves in the processing of non-adherent materials, researches have been conducted on hybrid microwave heating systems (MHH)which uses the concepts of conventional heating principles as well as microwave heating principles. The conventional heating process of the material first allows the surface heating and then takes place within the material with reduced thermal gradient. This can cause the microstructure of the surfaces to be poor, who in turn cause overheating or burning of the surface. In contrast to the conventional heating, in case of microwave heating, the core has poor microstructure due which there is thermal leakage.

In order to eliminate the differences in the temperature gradient of surface and temperature gradient of the core, researchers come up with a new approach called two-way heating or MHH in which the heating of materials takes place in both the direction, that is from inside and outside of materials. The various heating effects are shown in Figure 1.5.showing the temperature profile flattening by employing MHH in the sample. In microwave hybrid heating, uniform heating occurs along with the reduction in a temperature gradient. The above-mentioned features do not exist in conventional heating or microwave method.

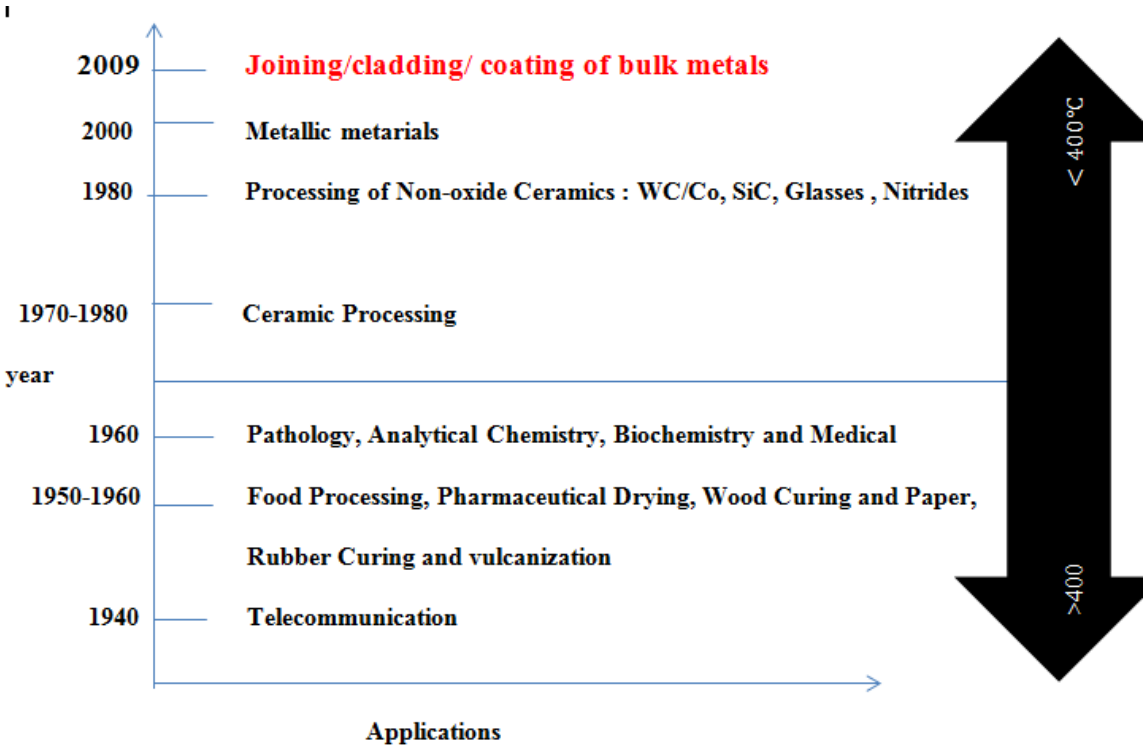

Figure 1.6.History of the development of microwave processing

The history of progress or growth in the area of microwaves is depicted in Figure.16 that shows the earlier progress was in the field of low-temperature applications. These developments were explored the elevated temperature applications also, mainly in the processing of ceramic specimens. The first literature review on the successful sintering of metallic materials, and studies have shown that fine powdered form of metallic materials can be coupled to microwaves [38]. Author successfully overcomes the challenge of processing of bulk metallic materials using microwave [39] in the form of joining by using a domestic microwave oven. This study has led to microwave applications for high-temperature applications. In recent years, applications for obtaining high temperatures by microwaves have been explored, and much research has been done in the area of materials coatings, cladding and using hybrid microwave heating.

Figure1.7. shows the progress in the area of processing of mass metallic materials utilizing microwave radiation.

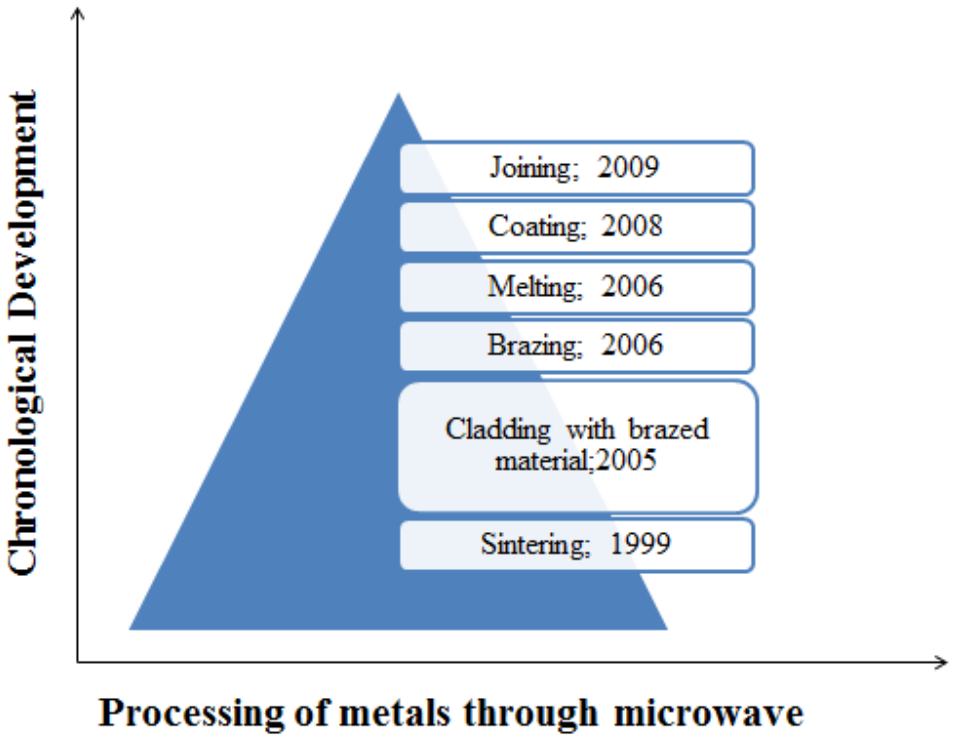

Figure1.7. Progress in the processing of metallic materials using the microwave energy

1.3.2 Advantages of Microwave Processing

The use of microwave energy in the heating process has several distinct advantages. The characteristic of lower energy consumption, together with higher heating rates and shorter processing times, has led to microwave heating as one of the difficult processes in the processing of materials. The foremost important advantages of microwave material processing include better microstructure, less defect formation, higher efficiency with less energy consumption and lower heating costs compared to conventional heating. Following are the advantage of the microwave process over conventional processes:

- **Microwave processing improves the mechanical properties**

Conventional sintering processes require elevated temperatures, higher heating rates, and this temperature is maintained for a fixed period. However, to maintain a uniform temperature distribution, the sample is generally maintained for a longer immersion period, that results in imperfections such as excessive particle growth, permeability, and cracking. Above mentioned problems can be overcome by utilizing a microwave processing technique that provides finer particle growth and relatively homogeneous

microstructures with improved properties in addition to shorter processing times. These desirable properties obtained because of rapid heating, constant heating of the material and shorter times to reach higher temperatures. The microstructures by the process are shown [40] in Figure. 1.8.

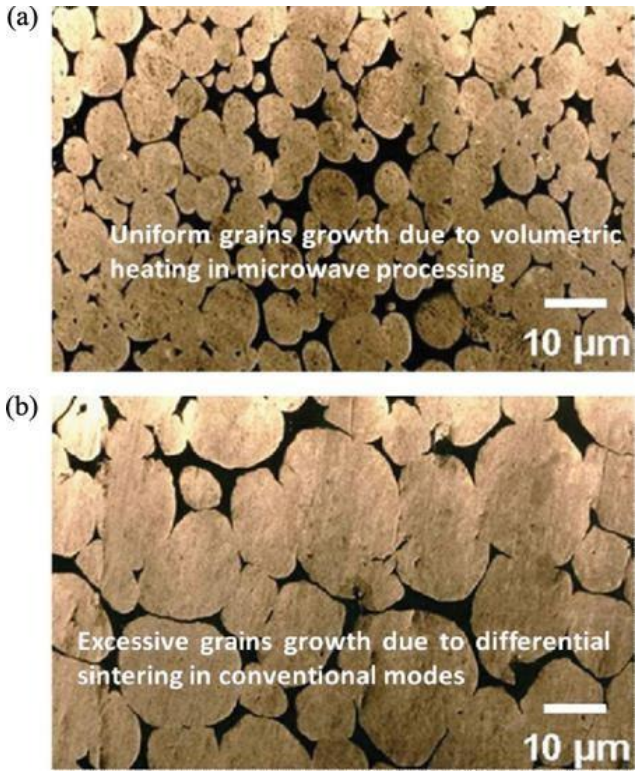

Figure 1.8 The microstructure of processed material by (a) microwave processing (b) Conventional processing [40]

- **Compaction parameters improved**

The density of the compact powder determines the properties of the final product. The greater the density of the processed material, the fewer defects is produced mainly in the porosity. Because of volumetric and uniform heating of the product, the densities achieved are greater for microwave or machined parts [41].

- **Fewer power consumptions**

In the microwave heating of materials, the radiation is absorbed directly by the sample which then converted into thermal energy and resulted in uniform heating of materials. It

has been reported in the literature that as compared to traditional material processing methods, microwave processing required 10 to 200 times less processing time and microwave heating consumes 10 to 100 times less energy respectively [42]. Due to the direct energy transfer, many losses are avoided, like the media for the heat transfer, the furnace heating, their walls. Transfer rate is also higher as compared to the conventional processes and also the high temperature can be achieved in less time which in turn reduces the total consumption of power for processing of materials shown in Figure 1.9.

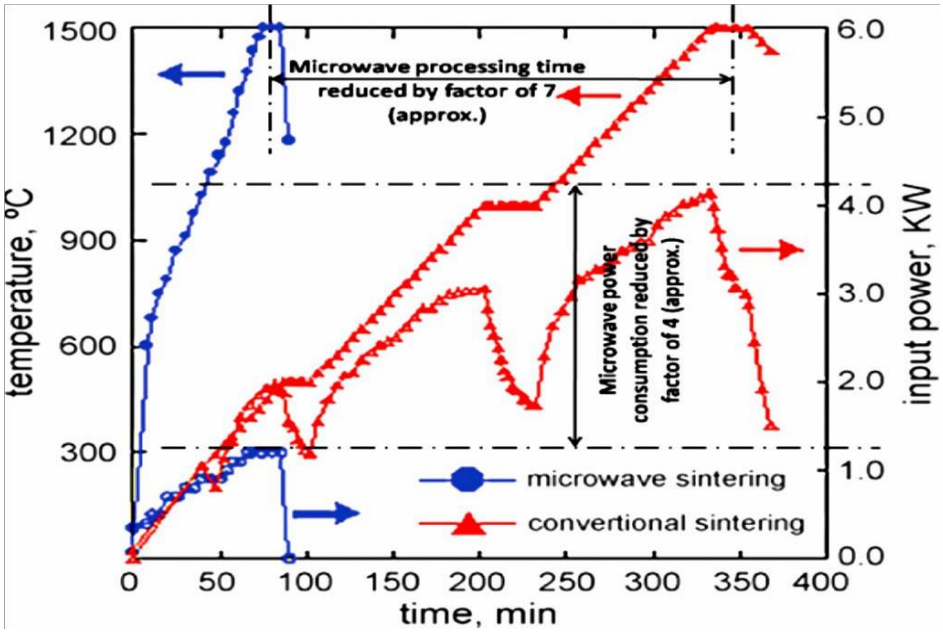

Figure 1.9 Power and processing time comparison during microwave and conventional sintering process [40]

All of these advantages have led to microwave material processing as a new technology in microwave processing and have improved research in this new field.

\

Chapter 2

Literature Survey

This chapter describes the different techniques used for dissimilar welding and the problems associated with them. Hot corrosion behaviour of materials, bimetallic weldments in different environments is also mentioned in this chapter. Researcher's for the long time trying to solve the problems. Decent success has also been achieved. A list of such work is thoroughly discussed in this chapter as literature survey and followed by research gaps.

2.1 Literature Review

Olivas et.al (2019) examined the detailed impact of the microstructure of a pre-shaped oxide scale on low-alloyed steel (Fe–2.25Cr–1Mo) when open to limited quantities of KCl(s). The examinations were completed for the environment produced by the burning of biomass and waste which is extremely intricate in nature [43].

Okoro et.al (2019) also recommended the development of materials that are corrosion resistant in biomass-based power plants as there are condensed deposits on the surface of the heat exchanger. These deposits attack the surface more severely which is completely different from the earlier traditional coal-based plants. Hence, they carried out a peroxidation treatment to improve the corrosion resistance of one of the nickel-based super alloys and found that peroxided Nimonic 80A showed better corrosion resistance as compared to the un-oxidized sample [44].

Li et.al (2018) tested super 304H austenitic stainless steel pre-coated in Na2SO4–25% NaCl mixture salt film in the air at a temperature of about 650°C and 750°C. They verified that the specific oxidation happens and a defensive oxide scale shapes at the early corrosion phase. The liquefy salts eliminate the integrity of the oxide scale and quicken hot corrosion of the alloy by the recurrent oxidation–chlorination during the further corrosion processing. Furthermore, inward sulfidation likewise adds to the corrosion of the alloy [45].

Reddy et.al (2019) explored the impacts of HCl and KCl, key species affecting biomass boiler corrosion, on a laser clad covering of the FeCrAl alloy Kanthal APMT. It was

discovered that HCl permitted chlorine-based corrosion to happen to recommend it can interact from the gas stage [46].

Arivazhagan et.al (2011) investigated AIS4140 low steel and AISI 304 steel dissimilar joints by electron beam welding (EBW), continuous Drive FRW and GTAW (DCEN). Microstructure part composition and mechanical properties were analyzed for each of the weldments. From the tensile result, electron beam welding (EBW) had the highest tensile strength (681Mpa) comparatively with Gas Tungsten Arc Welding (635 MPa) and Friction Resistant Welding (494 MPa) because failure for FRW happens at the aspect of AISI 4140 and for GTAW and EBW, the failure in AISI 4140 is ascertained at HAZ. Highest impact strength is observed in the sample welded by GTAW among the applied techniques [47].

Hosseini et.al (2016) discussed the weldability and microstructural of AISI 310/ metal 617 dissimilar welds by using DCEN GTAW. 12mm sheet of metal 617 and SS310 is taken and 3 fillers (ERNiCr3, ERNiCRMo1, and ER310) were selected. Welding parameters were selected as the current of 140Amp, Voltages range from 17-20V. Inconel 617 showed the best influence that causes resistance to crack due to natural action due to the quantity of left liquid film and solidification temperature ranges [48].

Hajiannia (2013) studied the properties (microstructure and mechanical) of low alloyed steel and 347 SS dissimilar weld joint ready by DCEN GTAW. The low alloy steel and AISI347 steel of thickness, length, an outside diameter of 8mm, 400mm, 200mm respectively. Two fillers(ER309L and ERNicr-3) are utilized with DCEN polarity and argon gas as shielding gas. Each weld joint is unsuccessful within the HAZ A335 in tensile testing. ERNiCR-3 provides the optimum mechanical properties of the dissimilar weld joint of Low steel and AISI347.All welded joints fail in the HAZ A335 in tensile testing. ERNiCR-3 provides optimum mechanical properties for dissimilar welded joints with low steel and AISI 347 [49].

Ramkumar et.al (2012) examined the result of different filler material on the performance of dissimilar weld joint of and Monel 400 AISI 304 made by GTAW. Therein experiment, E309L, and ENiCu-7 as filler are utilized. In that molten salt environment of potassium

sulfate and sodium chloride (60%) and cyclic air oxidation at a temperature of about 600 degrees. The reason for high-temperature corrosion in E309L welding is the micro segregation of Cu and Cr at the weld interface in the dendrite structure of the weld metal. Weld joints when subjected to the molten salt environment, corrosion rate increased. There is no change in weight in the environment of air oxidization [50].

Gupta et.al (2014) broaden the field of microwave material processing and build up another procedure for surface designing, known as microwave cladding. Authors had guaranteed that the microwave covering of tungsten powder on austenitic tempered steel substrates was created inside 120 seconds. The crack-free interface consists of the incomplete dilution of the stainless-steel substrate to a coating. It was stated that due to the existence of hard metallic carbides micro hardness value of cladding is higher in microwave processing. An average clad hardness of 945 ± 66 Hv was reported. Authors determined that the procedure of microwave cladding could grow as a new technology in surface engineering [51].

Bansal et.al (2014) used the radiations of microwave to develop the joints between bulk stainless and mild steel joints with the help of MHH technique. For the characterization of the joints developed by microwave processing route used for XRD,SEM, Vickers micro hardness. For forming the interface layer nickel powder of particle size 40 µm was employed. Joining of plates was confirmed by the backscattered electron images of the joints prepared by microwave processing [52].

Gupta et. al (2014) used the microwave energy to join the stainless steel, for that Ni-based powder was utilized for making the interface between the two metals. It was being reported that joint was crack-free but there was of porosity confirmed by microstructural analysis. It was also reported that as the content of nickel was increasing tensile strength was also increased [53].

Ramkumar et.al (2017) examined the impact of fillers in the pulse current gas arc welding of tungsten (PCGTAW) of Inconel 625 and Inconel 718. Fillers selected for joining the sheet of nickel-based alloys were ERNiCrMo-4 and ERNiCrMo-10. And it was found that parent metal Inconel718 has defects in both cases. Welds with filler ERNiCrMo-10 had better shock

resistance property interpreted by the impact test result. Hot corrosion studies had been dole out within the surroundings of artificial consolidated salt to 40% V_2O_5- 60% of Na_2SO_4 at the temperature of 900° C displayed that each metal 625 metal parent followed by the fusion space of ERNiCrMo-10 showed improved corrosion resistance in hot temperature environments. For the investigation of hot corroded speciessurface, analytical techniques were utilized [54].

Montgomery et.al (2018)studied the impact of the use of coatings in biomass-based power plant because the coating has different performance based on fuel mix and temperature and also studied how the microstructure changes with the time of course and temperature which can influence corrosion. It was concluded that the limits of the materials and the temperature limitations during the combustion of biomass (straw) were reported by the authors and the laboratory examination. Best performance was seen in the case of steel with chromium content between 15-20%. The steam temperature of 540 ° C was the maximum because above that there were extremely high corrosion rates and the initial work showed that the microstructure that developed during exposure [55].

Hashim et.al (2015) investigated the behaviour of oxidation of nickel-based superalloys for example Inconel 600 and Hastelloy C-22by determining an oxidation rate of the alloy in high temperature and ambient air. The method of cyclic oxidation was performed by heating the alloys periodically at a temperature of 900, 1000 and 1100◦C in still air and then cooled at room temperature. During the oxidation test, change in weight was measured. For the characterization of the oxide film formed on the surfaces of oxidized alloys, X-ray diffraction SEM were used. Inconel 600 and Hastelloy C-22 exhibited the ability to form a protective film of oxide. The film of oxide that deposited on both alloys was chromium oxide (Cr_2O_3) with a smaller quantity of mineral oxide $NiCr_2O_4$. The outcomes of the weight gain estimations suggest that the kinetics of the reaction of each alloy pursues the parabolic behaviour throughout the trial tests. Conjointly each alloy at 1100◦C displayed extreme spallation of an oxide film with linear decreasing within the weight modification estimations. The model of p-kp was enforced to explain the following cyclic method of spalling and growth of oxide [56].

Mortezaie et. al (2014)studied the mechanical properties, corrosion behaviour and microstructural properties of the joints. Joints developed between nickel based super alloy (Inconel 718) and austenitic stainless steel (310S) through TIG welding. Three different fillers were chosen, Inconel 82, Inconel 625, and 310 stainless steel . Results of microstructural study showed that microstructure of weld were completely austenitic for all the fillers. Joints produced by 310 and Inconel 625 filler metals showed the lowest and highest tensile strength respectively. Results of impact test revealed that weld of Inconel 82 had highest fracture energy. Coming to the corrosion behaviour of the fillers, Inconel 82 showed the best corrosion resistance amongst all confirmed by results of potentiodynamic polarization test. Author had concluded that the weld of Inconel 82 filler metal had the best properties at the ambient temperature [57].

Naffakh et.al (2009) worked to describe welding of AISI 310 austenitic tempered steel to Inconel 657 nickel–chromium super alloy. The welds were created utilizing four sorts of filler materials; the nickel-based comparing to Inconel 82, Inconel An, Inconel 617 and 310 austenitic stainless steels. That paper portrays the choice of welding consumables for the joint. The relative assessment depended on hot-breaking tests (Varestraint test) and mechanical properties estimations. As per Varestraint tests, Inconel A demonstrated minimal susceptibility to hot cracking /splitting. In strain tests, all weldments failed in the more fragile parent metals (i.e., Inconel 657). In addition, Inconel A weldments had the most astounding strength. Authors came out with an conclusion that Inconel A filler metal offered the best properties of the joints [58].

Wang et.al (2012) compared the two welding techniques namely tungsten inert gas welding (TIG) and metal inert gas (MIG). Dissimilar weldments of low alloy steel and duplex stainless steel were produced through the above cited techniques. Characterization of the weld joints were done by using SEM-EDS. Mechanical tests (Impact, tensile, micro hardness) and polarizations curves studied for the evaluation of corrosion behaviour of joints. Mechanical properties and better corrosion behaviour showed by MIG welding as more austenite exists in the weld metal. MIG welding showed higher resistance to Hydrogen embrittlement as compared to TIG welding .As cooling rate in MIG welding is low which resulted in wider fusion zone. Corrosion resistance of MIG welding in sea water is better than

TIG welding, as current density of MIG is lower. It was concluded that MIG welding has better corrosion resistance and mechanical properties over TIG welding [59].

Wu et.al (2015) used laser beam welding for the dissimilar weldments between low carbon steel (CS) and ferritic stainless steel. Two different speeds (12mm/s, 24 mm/s) were employed. X-ray diffraction, scanning electron microscope and optical microscope were used to examine the microstructure of dissimilar joint. Dissimilar joints had the micro structure of ferrite and martensite developed in the HAZ of carbon steel. As the welding speed increases, the width of HAZ of carbon steel becomes narrower. Ultimate tensile strength was same at the both welding speed, however, at a higher welding speed elongation is more [60].

Mittal and Sidhu (2018) studied the hot corrosion behaviour of joints of T91 and 347H , T91 HAZ in simulated environment of boiler. Characterization of the corrosion product was done by using SEM-EDS, XRD and X- Ray mapping. From the X- Ray mapping results it was found out that in T91,content of chromium is low because of the formation of carbides of chromium. T91 HAZ have poor oxidation resistance because of the presence of the carbides of chromium, martensitic,ferritic as well as martensitic morphology. Due to absence of protective phases and presence of non-protective oxides of Fe2O3 and Fe3O4, HAZ T91 experienced higher corrosion. Depletion of chromium occurred which cause higher corrosion [61].

Mittal and Sidhu (2015) employed Gas Tungsten Arc Welding (GTAW), Shielded Metal Arc Welding (SMAW) to produce dissimilar weldments. Fillers used were nickel based and austenitic. Comparison of microstructural features and mechanical properties obtained by the above two mentioned techniques. T91HAZ has higher Microhardness value due to the martensitic morphology. Tensile strength is higher in case of DTAW welding. Author concluded that gas tungsten arc welding with metal filler had showed far more better results for the weldments between 347H and T91 [62].

Ramkumar et.al (2014) used Pulsed Current Gas Tungsten Arc Welding with three different fillers namely ERNiCu-7, ERNiCrFe-3 and ER309L for joining AISI 304 and Monel 400. From the microstructural analysis, it was observed that all the weldments had the presence of

partially melted zone nearby the HAZ. Tensile strength was better in case of ERNiCu-7 filler metal as compared to ER309L and ERNiCrFe-3 filler metals. Weldments suffered extreme corrosion subjected to simulated environment of boiler due to the formation of non-protective (FeV_2O_4 and $CrVO_4$) scales [63].

Sharma and Gupta (2012) created cladding of EWAC + 20% $Cr_{23}C_6$on the substrate of austenitic hardened steel SS316 by utilizing microwave energy technique. The created claddings were characterized by different techniques like XRD,FE-SEM, EDS, and estimation of Vickers's smaller scale hardness. From the XRD results it was displayed the presence of Nickel iron, chromium carbide and nickel silicide phases that leads to the enhancement of hardness value of clads. Clads were successfully developed without any interfacial cracks. The microstructure of clads of cellular morphology. Micro hardness of clad is superior to the substrates. It was inferred that these claddings would be successfully utilized in wear opposition applications [64].

Srinath et.al (2011)broadened the work by joining of divergent metals through microwave energy. It was expressed that joining of different metals is a moderately troublesome errand because of contrasts in chemical compositions, thermal properties and mechanical properties.A nickel based powder with a molecule size of 40 µm was utilized for joining the substrates. The microwave joining of tempered steel (SS-316) to mild steel (MS) in mass structure was completed utilizing a multimode tool at 2.45 GHz and 900 W, utilizing charcoal powder as Susceptor material. The improved properties were accounted for due to the total softening and combination of the interface layer and complete fusion with the mass metals [65]

2.2 Research Gap

Many kinds of research has been done on dissimilar welding to the study the microstructural, mechanical properties and high-temperature corrosion behaviour with different welding techniques and different fillers but no research has been done on to study the tensile strength, microstructure, and high-temperature corrosion behaviour of Hastelloy C276 and SS304 dissimilar joints by utilizing microwave welding technique and Tungsten inert gas and the comparison of the properties obtained by the two techniques.

After intensive literature survey on microwave material process and standard TIG welding following gaps are reportable on that a lot of research will be done to widen this field of material joining to explore more practical and sensible applications.

1. The literature shows that no studies have been reported on the joining of dissimilar metal Hastelloy C276 and SS304 using microwave welding.
2. The comparison of microstructural properties, mechanical properties obtained by conventional TIG welding and microwave processed joints has not been reported so far for the selected materials system.
3. The literature shows that no work has been done on high-temperature corrosion properties of the Hastelloy C276 and SS304 joints developed by microwave energy and conventional TIG techniques in actual and simulated bio-fuel fired boiler environment.

2.3 Objective of Proposed Work

The literature review allowed the analysis of the research gap and to fulfil the above-mentioned gaps following research objectives has been defined

1. To join two dissimilar metals using conventional TIG welding and Microwave welding.
2. To study the microstructure and mechanical properties of dissimilar weldments obtained by TIG welding and Microwave energy Process.
3. To study the high-temperature corrosion performance of welded specimen under-simulated bio-fuel fired boiler environment and actual environment.
4. To compare the results of the joints obtained by microwave technique and conventional TIG welding.

Chapter 3

Methodology

3.1 Methodology

Research gaps were formed, and the purpose of this research was developed based on literature review. The following methodology was used to achieve the goal.

- In the first stage of work pilot experiments were carried out for joining the Hastelloy C276 and SS 304 by domestic microwave applicator. After performing hit and trial, the optimum processing time to process the actual joints which are about 8 min at 900 watts in the domestic applicator. For joining the two sample, a slurry of nickel powder put in between them and for protecting the joint from charcoal (Susceptor) by using a thin sheet of graphite.
- And in the second stage of work, Hastelloy C276 and SS 304 were welded by Conventional tungsten inert gas welding by using nickel electrode as filler.
- In the third phase, the samples were prepared by microwave and TIG technique for microstructural analysis and tensile testing. For microstructural analysis, samples were polished with emery paper of following grades 600, 800,1000, 1500, 2000, and 3000 followed by polishing with alumina paste on fabric wheel. For the tensile sample, E8 M-09 standard is used with a gauge length of 18 mm and width 3 mm.
- In the fourth phase, microstructural and mechanical characterizations were performed by utilizing the SEM, EDS, XRD, Vickers micro hardness, Tensile testing.
- In the fifth phase, hot corrosion tests were conducted in a simulated environment of molten
- Salts (60% K2SO4-60% Na2SO4-10%KCl-10%NaCl) and in the actual environment of biofuel based boiler.
- In the final phase of the work, a comparative assessment of both joining processes was performed to assess the quality of the joints obtained.
- Flow chart of all the phase of work is shown in Figure 3.1.

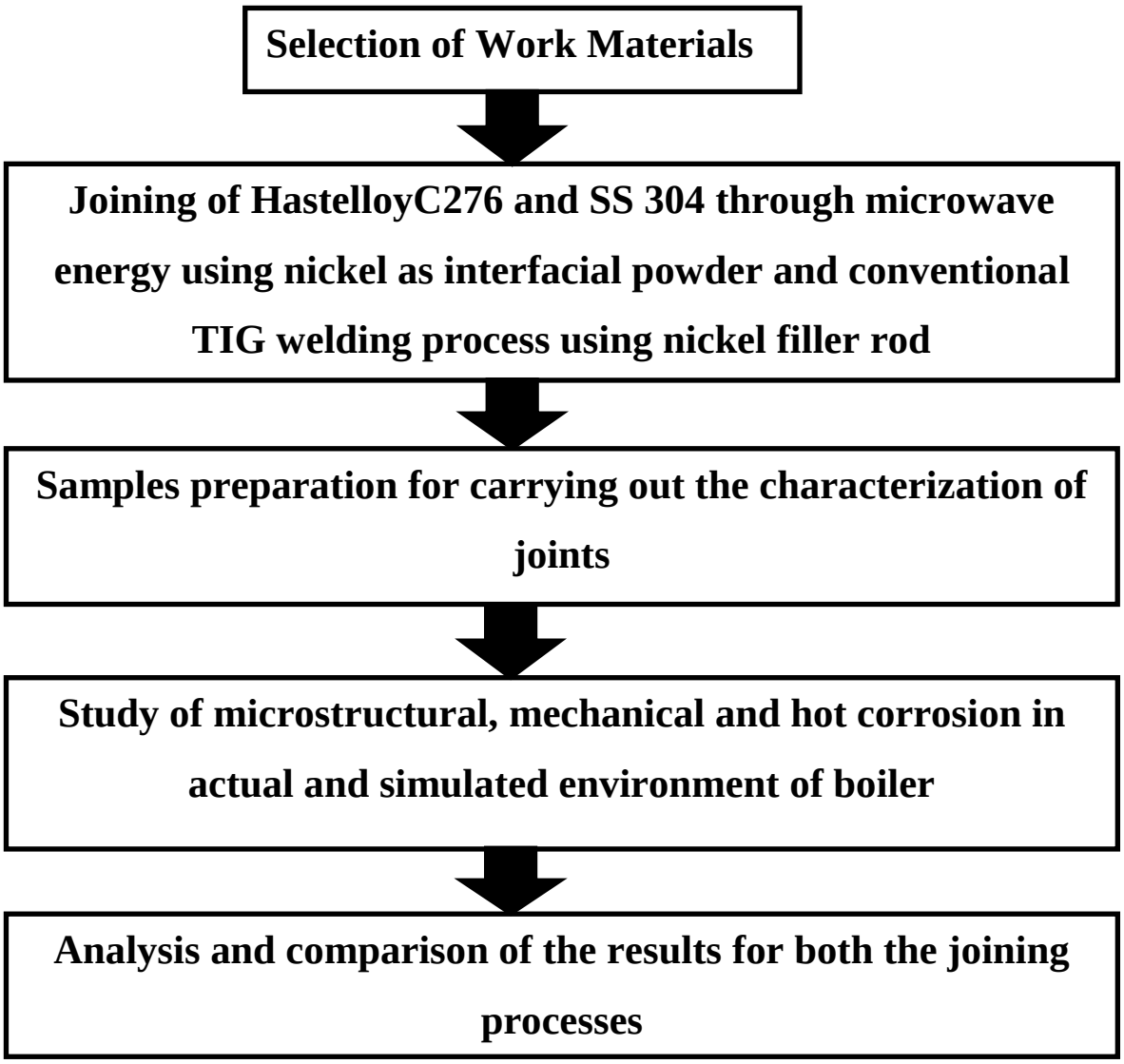

Figure 3.1.Flow chart of the methodology

3.2 Work Materials Selection

The material designated for joining process decided by literature survey which disclosed that stainless like SS-304 and corrosion resistance alloy (Hastelloy C276) are employed in several industrial applications together with automobile elements, aerospace components, marine applications, machines, and structural parts. These steels provide various benefits together with the improved life cycle, value performance, improved dependability, and lower maintenance. The effects of the addition of varied alloying components in these steels

improve several properties. Elements like nickel, molybdenum, chromium play a vital role whenever there is a requirement of corrosion resistance of high level. As chromium performs best in the oxidizing environment whereas molybdenum in reducing environment. A blend of each chromium and molybdenum provides the best protection against the pitting and crevice corrosion.

The chemical compositions of selected work materials. The chemical compositions of selected work material are presented in the Table3.1.

Table 3.1.Chemical composition of SS 304 and Hastelloy C276

Sr. No.	Materials	Elements Weight Percentage (Wt.%)					
		Ni	Fe	Cr	C	Mo	Others
1	Stainless steel (SS304)	8.59	60-67	18.2	0.08	2-3	1.24 Mn, 0.73 Si
2	Hastelloy C276	55-63	4-7	14..5-16.5	0.02	15-17	1Mn, 3-4.5 W

3.3 Welding Techniques for the Development of Joints

3.3.1 Joining Through Microwave Energy

Joining of SS 304 and Hastelloy C276 was done in domestic microwave applicator by applying the microwave hybrid heating technique.

For completing microwave joining, slurry of nickel powder and synthetic resin is applied at the faying surfaces specified on initial heating; the resin got evaporated from the joint region and leaving nickel powder.

Following are process parameters for joining of steels by using domestic Microwave as shown in table 3.2

Table 3.2. Process Parameters joining of steels by using microwave energy

Process Parameters	Descriptions
Microwave applicator	Domestic multimode microwave (Made: LG, Model: Charcoal)
Working frequency and maximum power rating	2.45 GHz and 900 watts
Exposure time	480 seconds
Work piece material	Stainless steel (SS-304) and Hastelloy C276
Interfacial powder	Nickel powder (40 µm average particle size)
Susceptor material	Fine grained charcoal powder
Separator material	99.9% pure thin graphite sheet

The schematic method of joining of steels by utilizing the microwave energy is shown in Figure 3.2 and 3.3

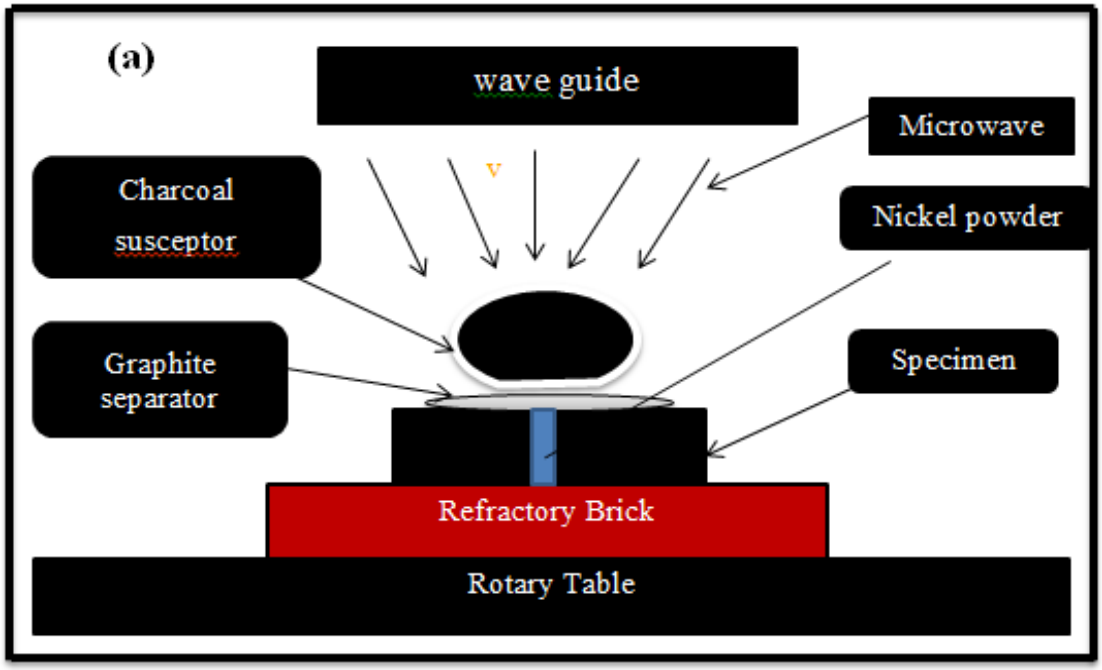

Figure 3.2: Schematic of the process of joining through microwave energy

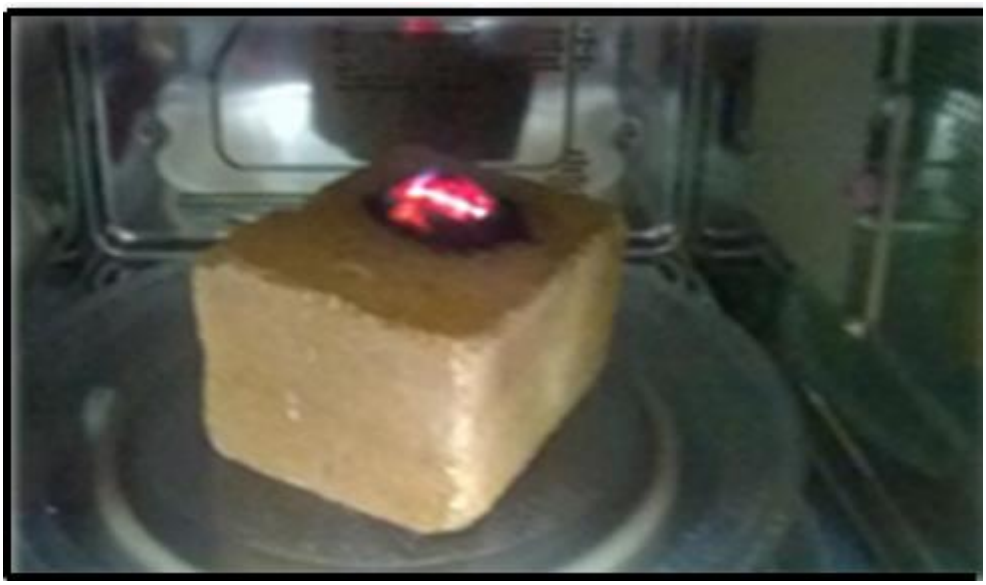

Figure 3.3 Actual joining of steels by microwave energy

3.3.2 Joining through Conventional Tungsten Inert Gas (TIG) welding

Gas Tungsten Arc Welding also is known by the name Tungsten Inert Gas (TIG). It is one type of arc welding in which a tungsten electrode is utilized for the joining purpose. Tungsten electrodes are used because they can withstand very high temperatures without being damaged and minimized without melting or erosion. In GTAW, for joining the metals, heat is applied that melts the work piece, due to established arc between work piece and electrode them and then joining occurs. Here for joining the stainless steel (SS 304) and Hastelloy C276 nickel filler rod is utilized. For shielding the weld pool, argon and helium are used for the same. Argon as compared to helium ionized more easily so the arc initiation is. The oxidizing cleaning action is more by argon than helium.

Table 3.3: Welding Parameters

Welding Current	80 Amps
Filler wire	ERNiCrMo3
Groove type	V design
Polarity	DCEN
Shielding gas	Argon, Helium
Pass	Multiple

Figure 3.4.TIG welding set up [Photo courtesy: TIET, Patiala].

Applications

- Aircraft
- Food processing industry
- Automobile industry
- Precision manufacturing industry
- Nuclear industry

3.4 Preparation of Laboratory Experiments

3.4 Heat treatment of boats

The boats of alumina, which can withstand at high temperature, were undergone through the heat treatment process at a temperature about 750° C for 24 hours in a laboratory furnace, in order to remove the moisture if. The purpose of the heat treatment of the boat was to maintain the constant weight of the boat.

3.5 Preparation of sample for hot corrosion test

TIG welded sample and Microwave joined samples were polished to get a uniform surface by removing the impurities. Before performing the experiment, dimensions like height, length, breadth were measured with the help of digital vernier calliper.

3.6 Hot Corrosion Study under Simulated Environment of Boiler

Studies of high-temperature corrosion were done in an environment of molten salt (Na_2SO_4, K_2SO_4, NaCl, and KCl) for 25 rounds under the cyclic condition. High-temperature corrosion can be defined as accelerated corrosion because of the presence of the salts species like NaCl, Na_2SO_4, K_2SO_4 that conglomerate to form the deposits of molten, which are responsible for the loss of the protective layer of oxides. Hot corrosion generally takes place in the temperature range of 700-900° C in the presence of sulphates compounds. At elevated temperature, deposits of molten salt (Na_2SO_4) can have an adverse effect on metal. In this particular study, an environment of molten salts was simulated for biofuel-fired atmosphere (40%K_2SO_4- 40%Na_2SO_4 -10%KCl-10%NaCl). Before placing the samples in a laboratory furnace, a uniform coating of salt of the thickness of 3-5 mg/cm2 were applied on the preheated samples (250 °C) with a camel hairbrush. For the study of hot corrosion, each cycle's time duration of 1hr of heating furnace followed by cooling of samples for 20 min at ambient temperature.

3.7 Study of Hot Corrosion under Actual Environment of Biomass Fired Boiler

As the non-renewable energy sources are depleting at a fast rate, so as substitute biomass has become one of the most generally used as an energy source. Biomass includes all the by-products of agriculture like wood, husk, agricultural residue. In a way biomass also helps in reducing the greenhouses gasses and it also reduces the dependency on fossil fuel for producing electricity. Biomass is cheap, easily available. In most of the power industries rice husk, one of bio-fuel used as an energy source. Besides the advantages, husk has another side too that is, on burning the husk environment of boiler get contaminated due to the production of salts and these salts get deposited on the surface of the components and degrade the oxides layer. As a result life of the component decreases. So external protection is needed to protect the component. Study of high-temperature corrosion performed in the actual environment of

the boiler. The plant where the study was done is in the name of Necter plant located in the DeraBassi, Punjab. Two samples, one of TIG welded and one of microwave joining were hanged inside the boiler by using A-grade kanthal wire (heat resistant) at temperature about 750±50 °C. Samples were there in for 100 hours, XRD and SEM-EDS analysis were done for the characterization. Samples before placing into the boiler are shown in Figure 3.5

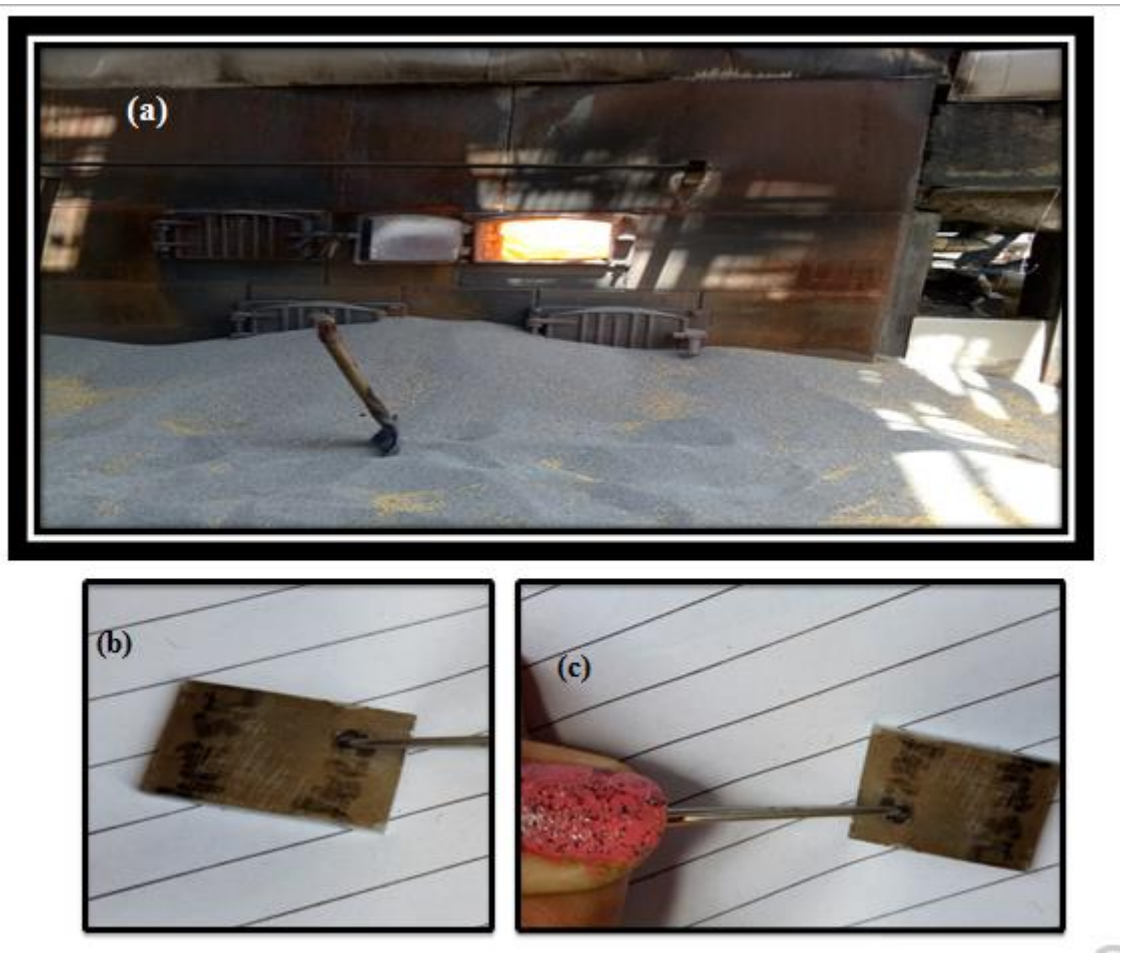

Figure 3.5 (a) Boiler (b) Microwave sample (c) TIG sample

3.8 Techniques for Characterization

The word characterization in material science refers to the processes by that the materials microstructure, properties, and correlation between structure and properties are investigated and measured. There are numerous characterization techniques out there that are being practiced for hundreds of years, whereas a number of them emerged recently. The techniques utilized in this work for characterizations of microstructure and mechanical properties are concisely represented in this section.

3.8.1 X-Ray Diffraction (XRD)

X-ray diffraction abbreviated as XRD and is used to identify the phases of the crystalline material. It is helpful in evaluating minerals, polymers, composites the product of corrosion, also for unknown materials. XRD principle is based on the Bragg's Law, whose equation is $n\lambda = 2d\sin\theta$. Bragg's law gives the relationship of a wavelength of electromagnetic wave with the lattice spacing and diffraction angle in a crystalline material. Since each mineral has a set of distinctive d-spacing and the conversion of the diffraction peak to d-spacing permit mineral identification.

3.8.2 Scanning Electron Microscope (SEM) equipped with Energy Dispersive X-ray Spectroscopy (EDS)

Scanning electron microscope equipped with energy dispersive x-ray spectroscopy is used to get information about the morphology of the samples prepared by microwave joining and TIG welded. To know the compositions of elements at different spectrum EDS is done. Secondary Electron Image and X-Ray mapping were done for the cross-sectional analysis.

Figure 3.6 SEM equipment equipped with EDS (Photo courtesy: SAI Labs, TIET, and Patiala)

3.8.3 Vickers Micro hardness Test

The Vickers micro hardness test was invented by George Sand land and Robert L. Smith at Vickers Ltd. As compared to another hardness test, the Vickers hardness test is easier. Vickers micro hardness test can be used for all materials of any hardness value as it is

independent of the indenter. It can be used for a wide variety of metals.The unit in which Vickers micro hardness test measured is Vickers Pyramid Number (HV) or Diamond Pyramid Hardness (DPH). In this work, it is used to measure the hardness value of the joint of samples processed through microwave Joining and TIG welding technique. Vickers micro hardness tester is shown in Figure 3.7.

Figure 3.7Vickers Tester (Photo courtesy: Mechanical Department, TIET, and Patiala)

3.8.4 Tensile Testing

One of the fundamental material tests is a tensile test in that material is subjected to a particular load until the material fails. The data obtained from the tensile test contains information regarding yield strength, ultimate tensile strength, reduction in area and maximum elongation. From the ASTM standards, available tensile tests carried out. In the present work standard which is being used is ASTM E8/E8 M-09. The dimension of the sample is shown in the Figure 3.8 (a) according to the ASTM E8/E8 M-09 standard and tensile tests carried out on Zwick-RoellZ010 universal testing machine with the strain rate of a 0.083 mm/s. Equipment of tensile testing is shown in Figure.3.8 (b).

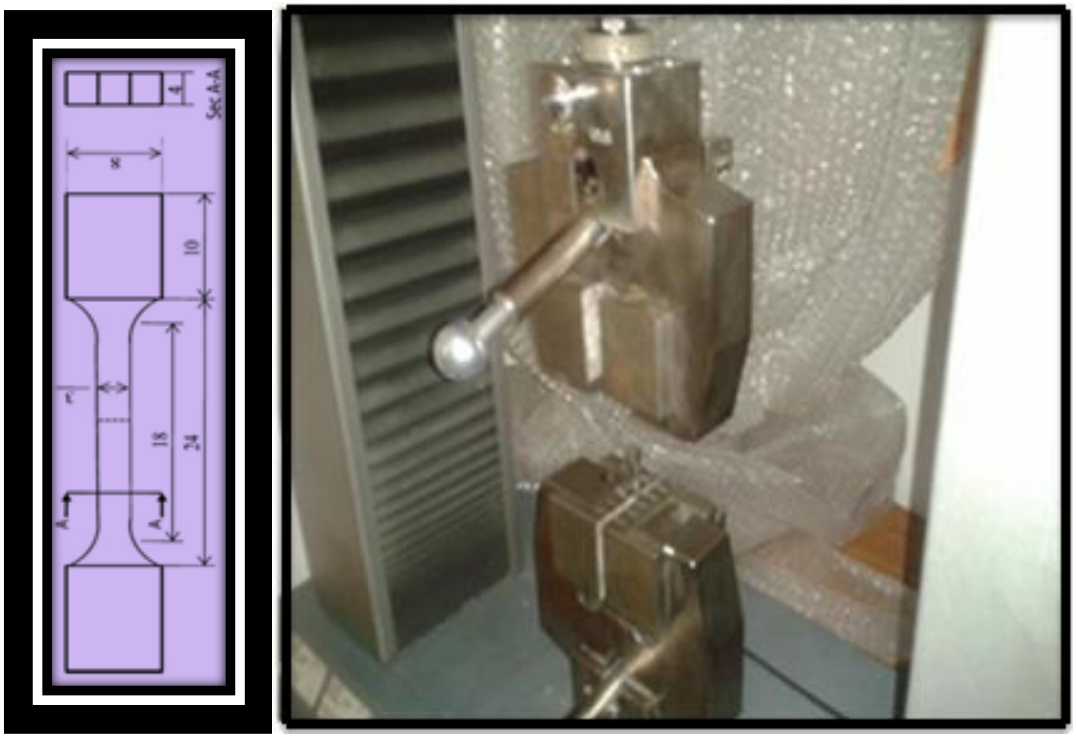

Figure 3.8 (a) Standard tensile test specimen (all dimensions are in mm) (b) Tensile testing machine (Photo courtesy: Chemical department, TIET Patiala)

Chapter 4

Results and Discussions

In this particular chapter, all the experimental and characterization outcomes of the joints developed between SS304 and Hastelloy C276 by conventional inert gas welding technique and microwave hybrid heating is presented. Comparison of the microstructural results, tensile strength results and high-temperature corrosion resistance results obtained by the two above mentioned joining techniques is discussed.

4.1 Characterization of Nickel Filler Rod and Nickel Powder

Joining through microwave energy was achieved by applying the powder of nickel in the form of slurry between the two metals. The morphology of the nickel powder is in the spherical form having an average size of 40 µm and is confirmed by the SEM of the nickel powder. SEM image of the nickel powder is shown in Figure 4.1

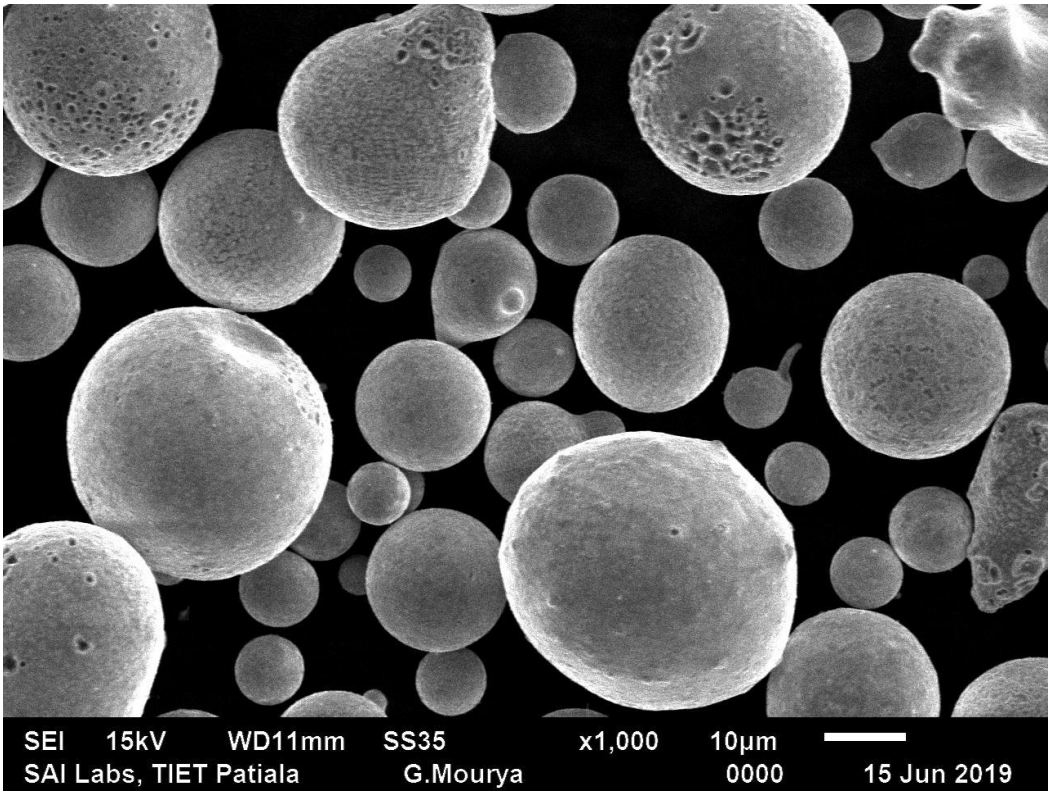

Figure 4.1 SEM image of nickel powder showing spherical morphology

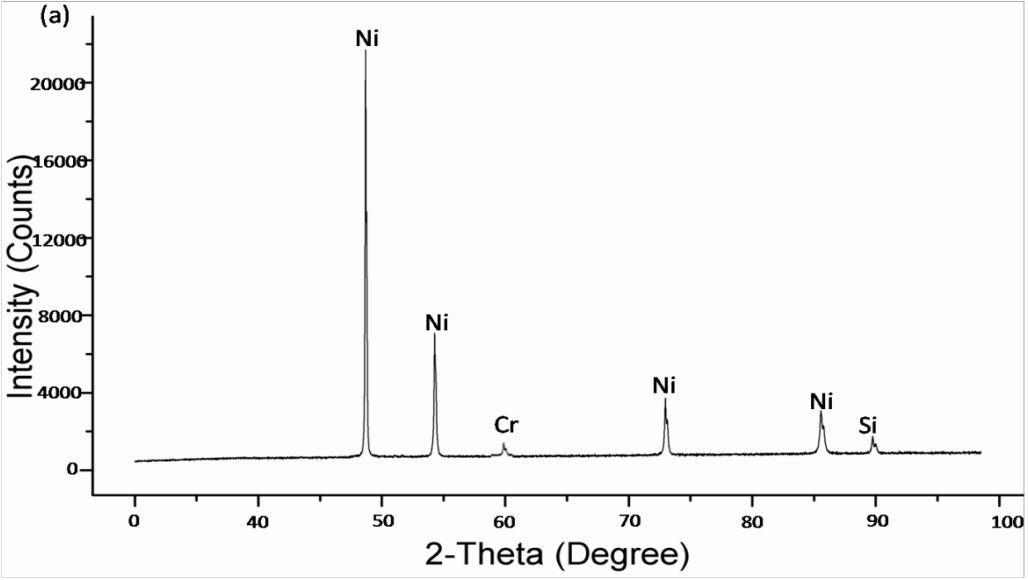

Figure 4.2: Typical XRD pattern for nickel powder used for microwave joining

In the TIG welding, joining of two plates of steel namely SS304 and Hastelloy C276 by using nickel filler rod and the EDS of the filler rod is shown below in Figure 4.3 and it can be clearly seen that the main constituent is nickel along with chromium.

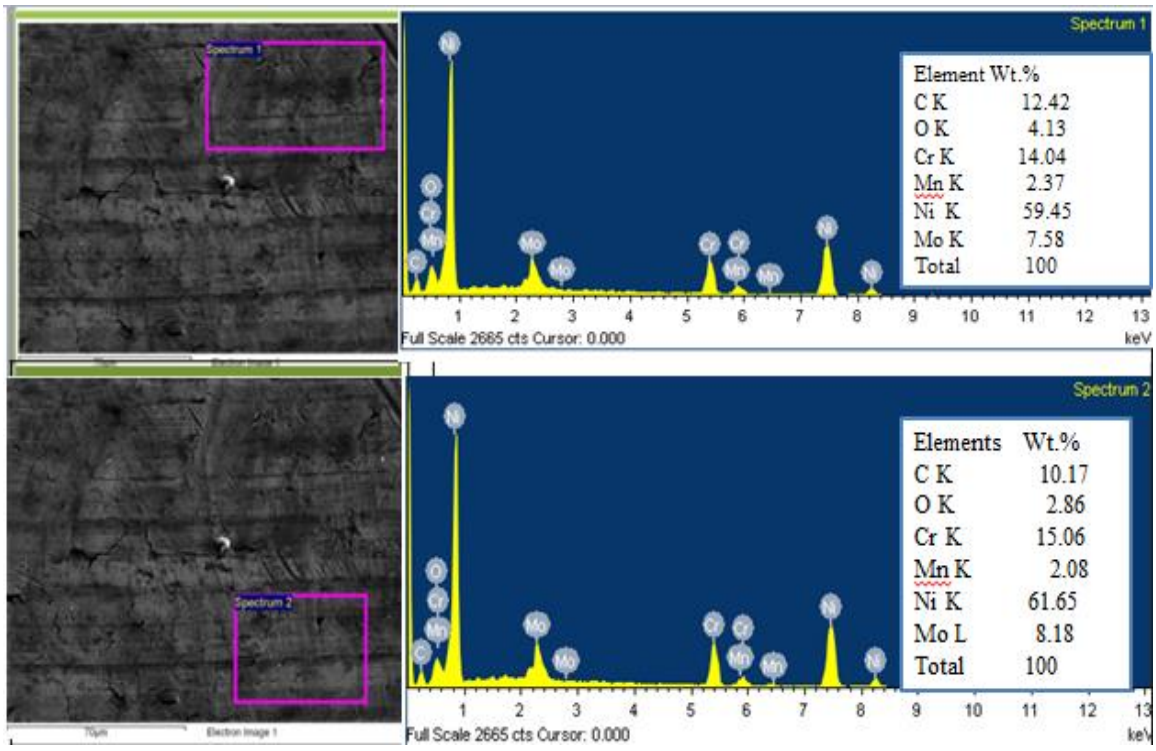

Figure 4.3: EDS of nickel filler rod

4.2 Characterization of Joints

The TIG-welded joint (Figure 4.4a) and microwave processed joint (Figure 4.4b) of SS-304 and Hastelloy C276.Characterizations of these joints were done using XRD, SEM along with EDS analysis at the cross-sections of the joint.

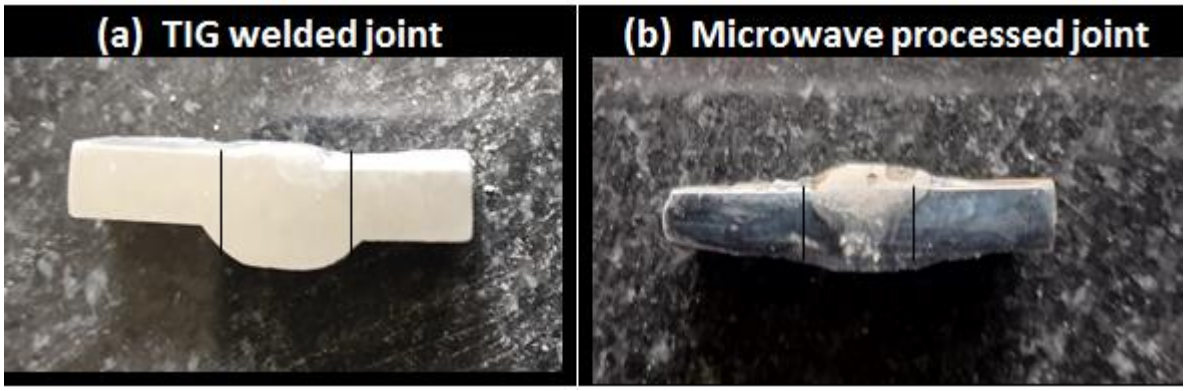

Figure 4.4: Joints of SS304 and Hastelloy C276 by (a) TIG welding and (b) Microwave joining

Before the characterization, preparing of samples was done, first by cutting the sample by low-speed diamond cutter followed by polishing the samples with the emery paper of grades 200, 600, 800,1000,1200,1500, 2000, 2500, and 3000. Final polishing was done by disc polisher with alumina paste and was put in a plastic bag to avoid any unwanted contamination of joints.

4.2.1 Microstructural Analysis of Joints

SEM images of weld bead and base metals of the sample joined through microwave energy is shown in Figure 4.5.

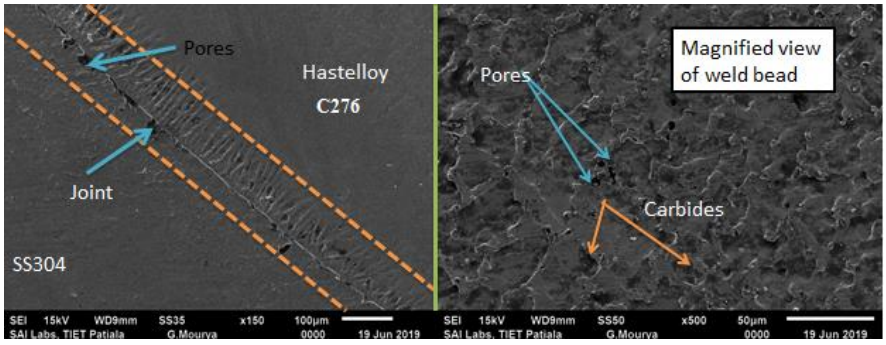

Figure 4.5: SEM micrographs of joint of microwave joined sample

Joining of Hastelloy C276 and SS304 is successfully done through the microwave heating,

can be seen in the SEM image shown in Figure 4.5. At higher magnification, SEM micrograph shows the uniform microstructure of the weld bead.From the EDS analysis, it is very clear that cells of joint are rich in nickel and iron whereas interfaces are rich in carbides (nickel, iron, and chromium) shown in Figure 4.6.

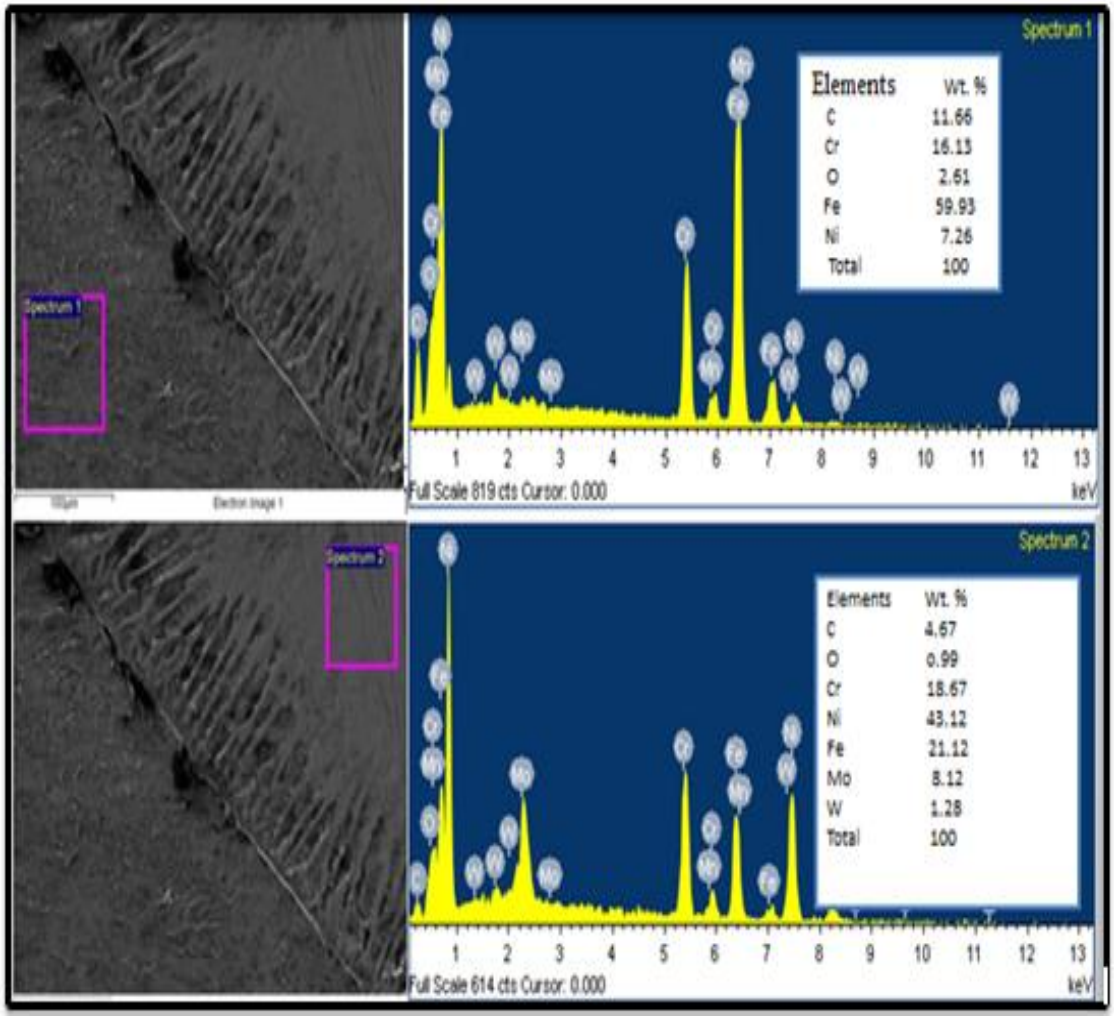

Figure 4.6 EDS of the sample prepared through the microwave energy.

SEM Micrograph of TIG welded sample is shown in Figure 4.7. Joining of the SS304 and Hastelloy C276 is successful by the TIG welding which is visible in the Figure4.7. The SEM Micrograph showing that pores is present in the weld zone of the bimetallic joints. This may be due to the fact that gases get entrapped during the welding.

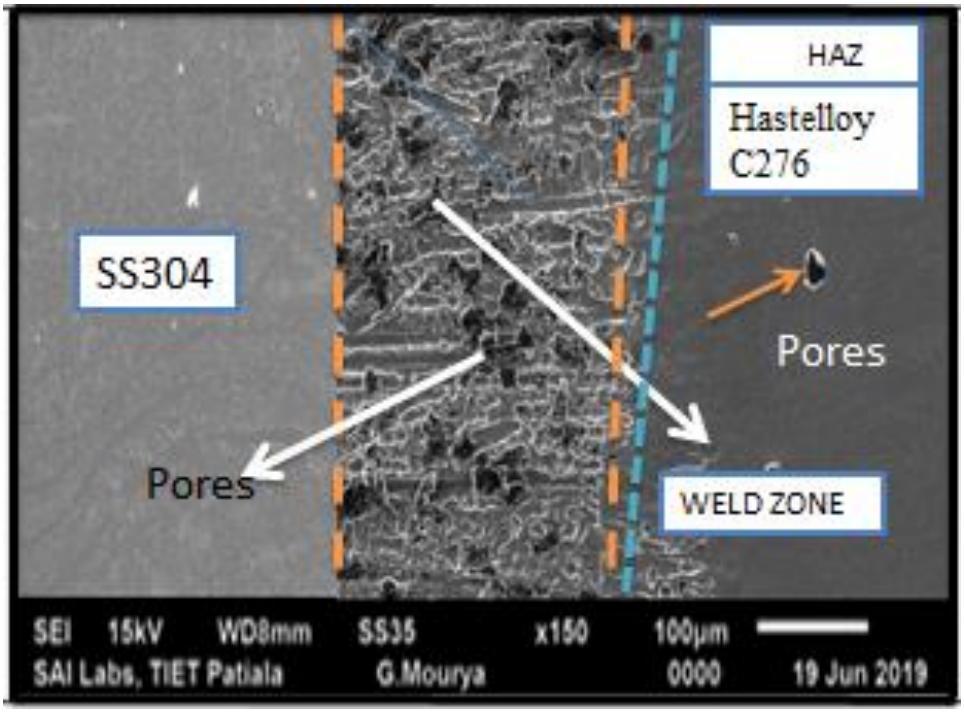

Figure 4.7 SEM image of TIG-welded sample

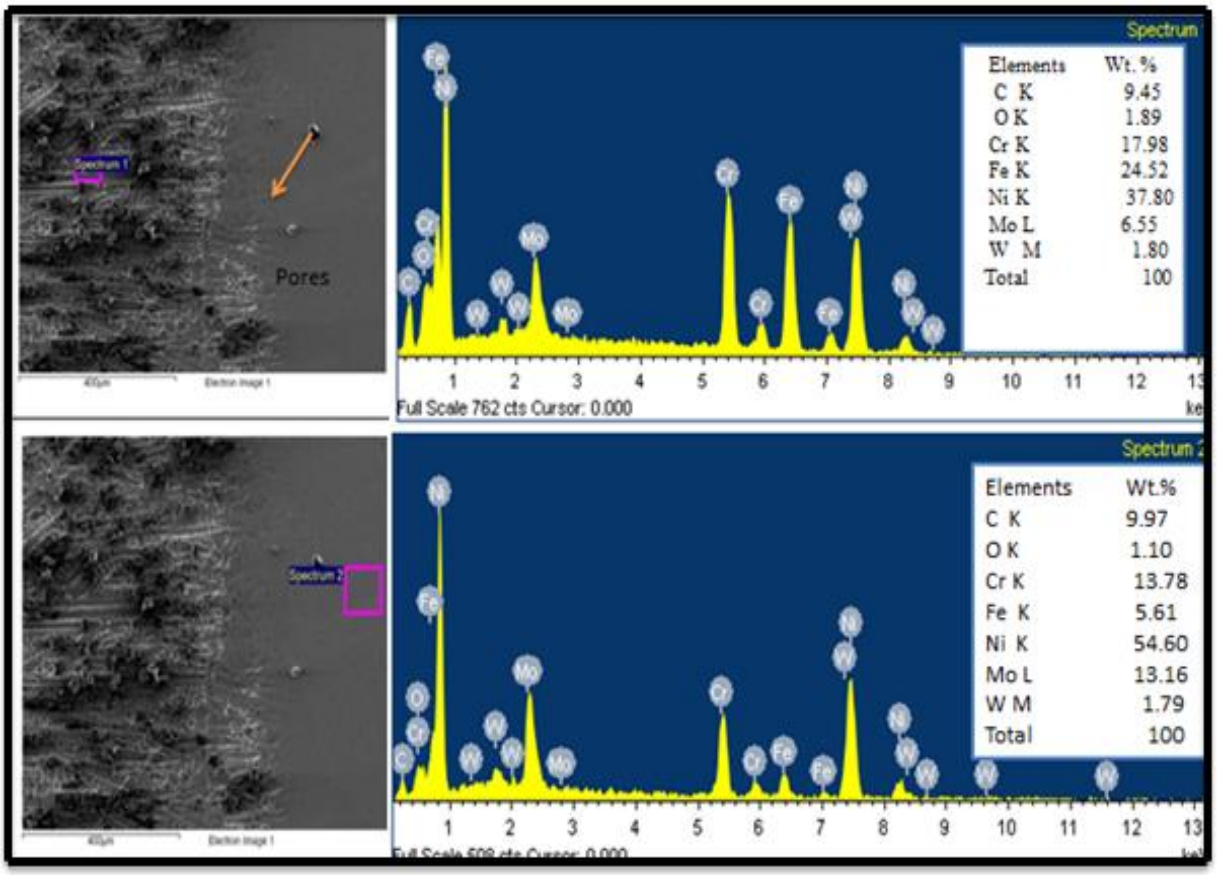

Figure 4.8 EDS of TIG-welded sample

4.2.2. XRD Analysis of Joints

XRD spectrum of microwave prepared joint of SS304 and Hastelloy C276 are shown in Figure. 4.9, which was gotten by setting nickel powder at the interface. Fusion of powder with the base metals is being confirmed by the iron phases present. Some carbides are formed such Fe_3C, Cr_7C_3. XRD spectrum of the joint between SS304 and Hastelloy C276 prepared by conventional TIG welding technique shown in Figure 4.10, which was gotten by using a nickel rod as a filler. Phases present are Fe_2O_3, $NiMnO_4$, FeNi, Fe, and C.

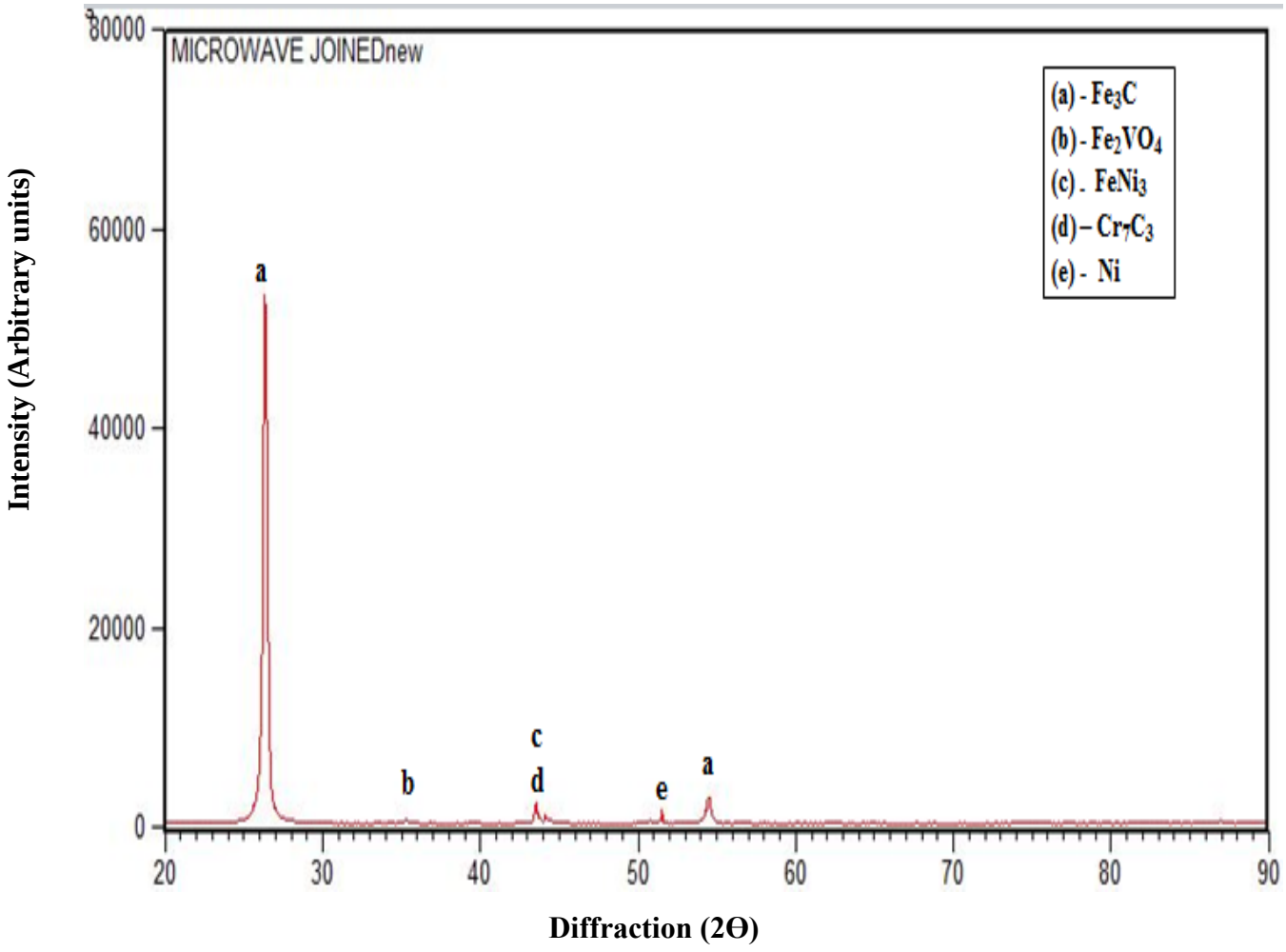

Figure 4.9 XRD spectrum of microwave processed joint

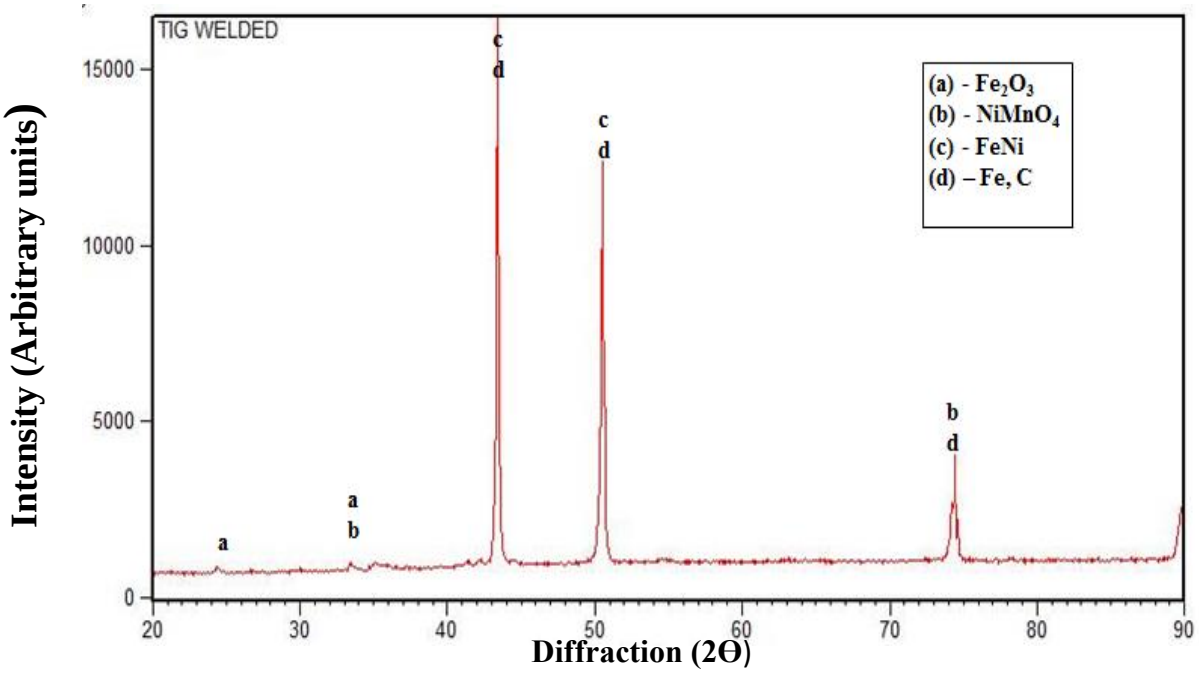

Figure 4.10: XRD spectrum of TIG-welded joint

4.2.3 Mechanical Characterization of Joints

For mechanical characterization of joints, Vickers micro-hardness and tensile testing were carried out for the evaluation of the strength of joints formed by TIG welding and Microwave joining. The results of the Vickers hardness of the samples are shown in table 4.4 along with indentations images in Figure.4.11.

Table 4.1: Vickers micro-hardness tests readings

Material	Vickers Micro-hardness (HV)				
	Base Metal	TIG Welded		Microwave Processed	
		Interface	Joint	Interface	Joint
SS-304	225±5	264±5	295±10	245±5	348±10
Hastelloy-C276	320±5	388±5	389±10	368±5	410±10

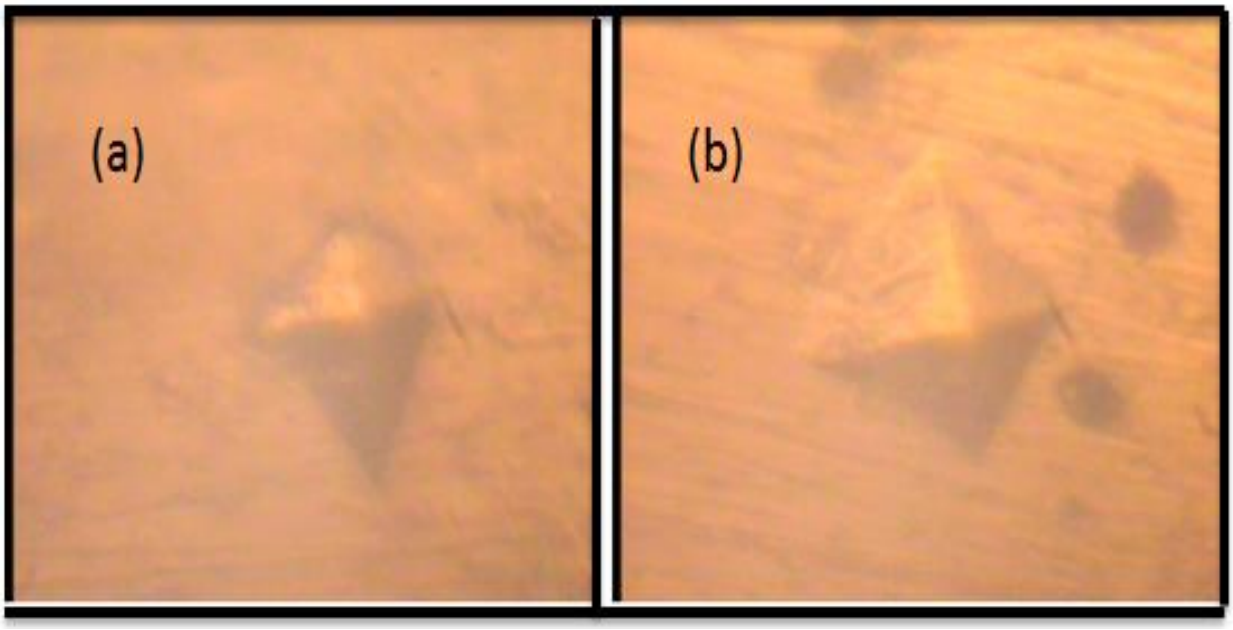

Figure 4.11 Diamond indent on (a) Joint on Sample joined through Microwave energy (b) Joint of TIG- welded sample.

From the Vickers micro hardness value, it is interpreted that in both joining techniques, the hardness value at the joint is higher because of the presence of carbides. In TIG welding, hardness at the interfaces is higher than microwave joining because of the tungsten's presence in the microstructure. Whereas the hardness value at the joint in case of microwave joining is better than TIG welding because of the presence of carbides in the joint region. Indentation resistance within the joint region is higher because of the tougher phase, however deeper and elastic indentation is created on the parent metal surface. Ultimate tensile strength (UTM) and % elongation are presented in Table 4.2 after the joints subjected to tensile testing.

Table 4.2: Results of the tensile strength of joints

Material	**Microwave Processed Joint**		**TIG Welded joint**	
	σM (MPa)	**% Elongation**	**σM (MPa)**	**%Elongation**
SS304-Hastelloy C276	**379**	**1.5**	**325**	**4.5**

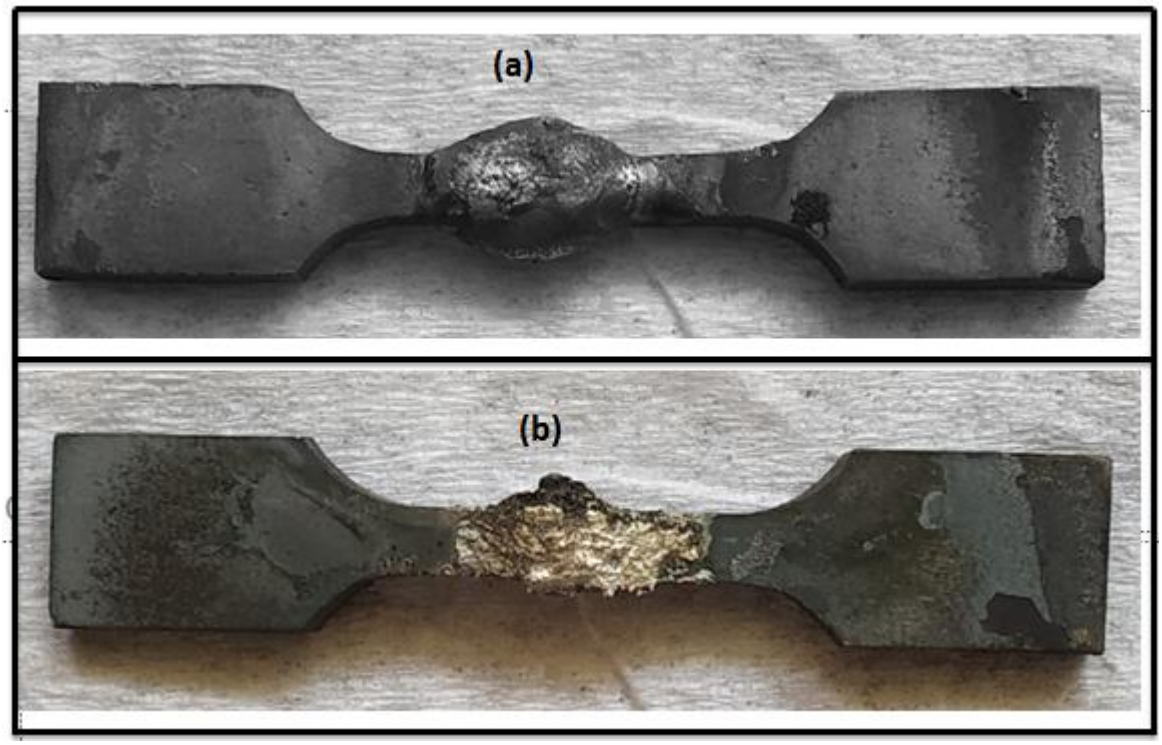

Figure 4.12 Tensile samples of (a) TIG welding (b) Microwave energy

From the results of tensile testing, it is concluded that the tensile strength of the joint of microwave processed sample is far better than that of the TIG welded joint.The conceivable reason behind a higher quality of microwave joints might be lower imperfections like porosity and breaks, better dissemination of nickel powder with the base metal. If we look at the results of the percentage elongation of joint of TIG-welded sample has more elongation than the joint of microwave processed sample.

4.3 Hot Corrosion test

4.3.1Hot Corrosion Study in Simulated Environment of Boiler

4.3.1.1 Visual Examination

Microwave joined and TIG welded samples were subjected to an environment of the molten salt of 40%Na_2SO_4-40%K_2SO_4 -10%NaCl-10 %KCl in laboratory at 750°C. After each cycle photos were taken for the visual inspection. After the first cycle of test, oxide of fragile nature was observed and oxide of greenish colour is seen on the surface of the microwave joined sample. Green coloured oxide depicts the formation of nickel oxide, as the joint is prepared with pure nickel powder. As the number of cycle increases corrosion rate also increased

which can be seen in the images shown in Figure. 4.13. In the 25th cycle, more porous and fragile oxides formed along with the spallation of oxides as shown in Figure 4.13 (d).

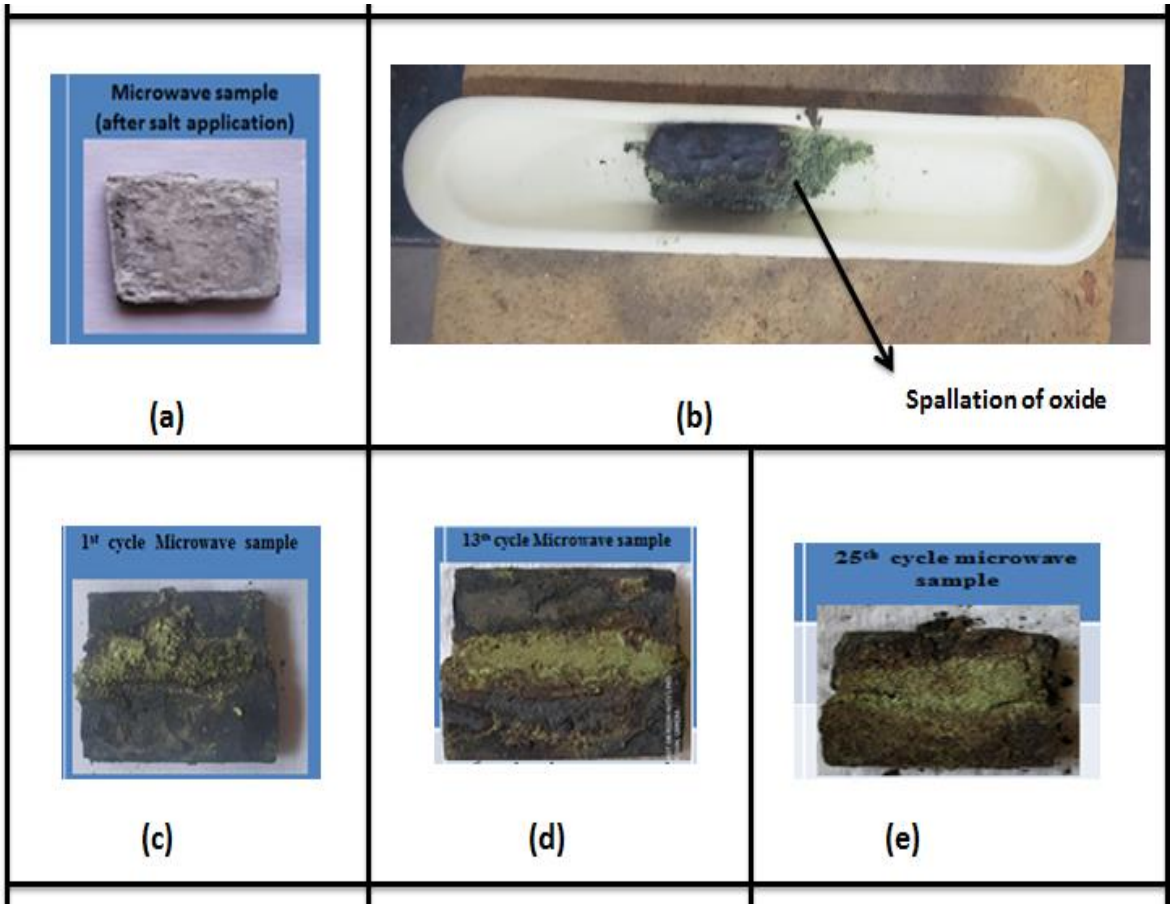

Figure 4.13 Macro photos of Microwave joined subjected to simulated environment of boiler at 750° C (a) Sample after salt application (b) Spallation of oxides (c) 1st cycle (d) 13th cycle (e) 25th cycle

In the case of TIG-welded sample, 1st cycle, 13th cycle and the 25th cycle of hot corrosion test are shown in Figure 4.14. It is observed that after the 1st cycle minor spallation is seen along with reddish brown oxide on the surface of TIG-welded sample due to the formation of iron oxides which was also reported by [46]. In the subsequent cycle oxides colour changes to the dark grey, this depicts the presence of chromium oxides.

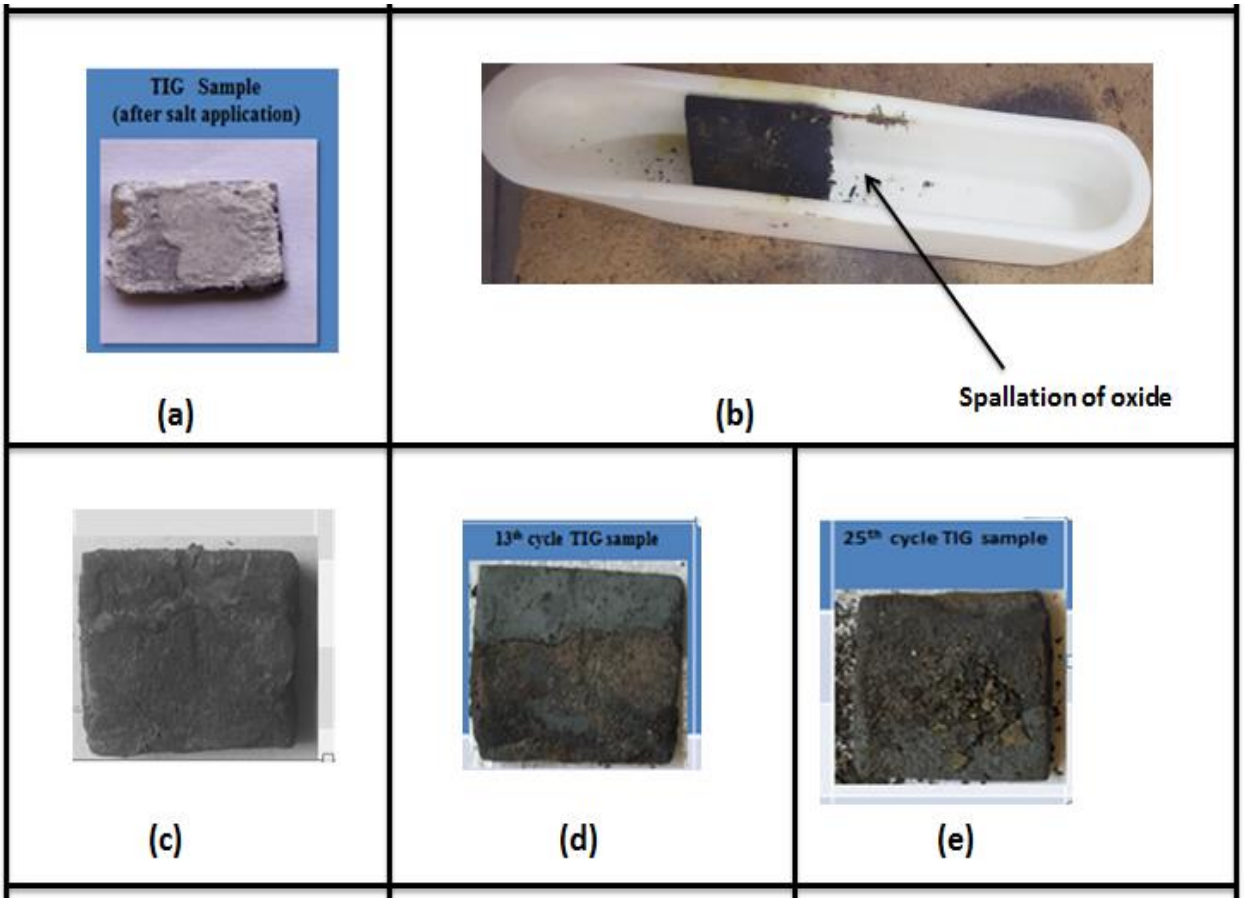

Figure 4.14 Macro photos of TIG-welded sample subjected to simulated environment of boiler at temperature 750° C (a) Sample after the salt application (b) Spallation of oxides (c) 1st cycle (d) 13th cycle (e) 25th cycle.

4.3.1.2 Weight Change Measurement

Weight change if any was noted down after every cycle of exposure. A graph has been plotted between the Weight change/Surface area Vs Number of cycles and is shown in Figure 4.16. It was observed that both the samples undergone through weight loss.It is being observed that both the specimens follow nearly parabolic rate law. The parabolic rate constant, Kp, calculated by a linear least-square algorithm to a function in the form of $(W/A)^2$ = Kpt,, in the equation W/A represents weight change per unit surface area (mg/cm^2) and t is no. of cycle. Weights of both the samples were recorded after each cycle from the 1st cycle to the 25th cycle.

Initial wt.	8.4374 gm	8.2381 gm
Wt. after salt application	8.4840 gm	8.2812 gm
Cycle No.	(Wt. in gm) Microwave Sample	(Wt. in gm) TIG sample
1	8.4668	8.2939
2	8.4596	8.2737
3	8.4582	8.2326
4	8.4465	8.1087
5	8.4448	8.0994
6	8.4354	8.0886
7	8.4293	8.0747
8	8.4286	8.0643
9	8.4201	8.0598
10	8.3986	8.0466
11	8.3901	8.0490
12	8.3802	8.0484
13	8.3701	8.0480
14	8.3690	8.0365
15	8.3665	8.0301
16	8.3603	8.0001
17	8.3540	7.9987
18	8.3470	7.9923
19	8.3345	7.9895
20	8.3213	7.9888
21	8.3176	7.9815
22	8.3096	7.9704
23	8.2970	7.9625
24	8.2540	7.9500
25	8.2345	7.9593

Figure 4.15 Measurement of change in weight of microwave processed sample and TIG welded sample after each cycle run

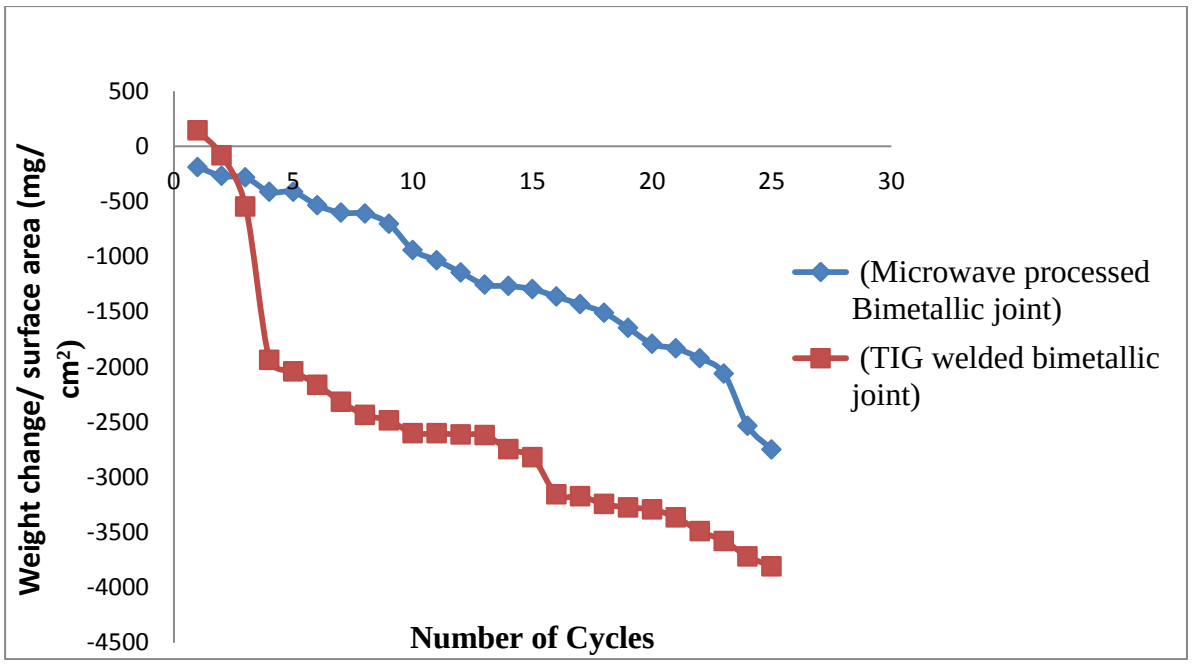

Figure 4.16 Plot of Weight change/surface (mg/cm^2)areas against the number of cycles in the simulated environment of boiler for 25 cycles at 750 °C.

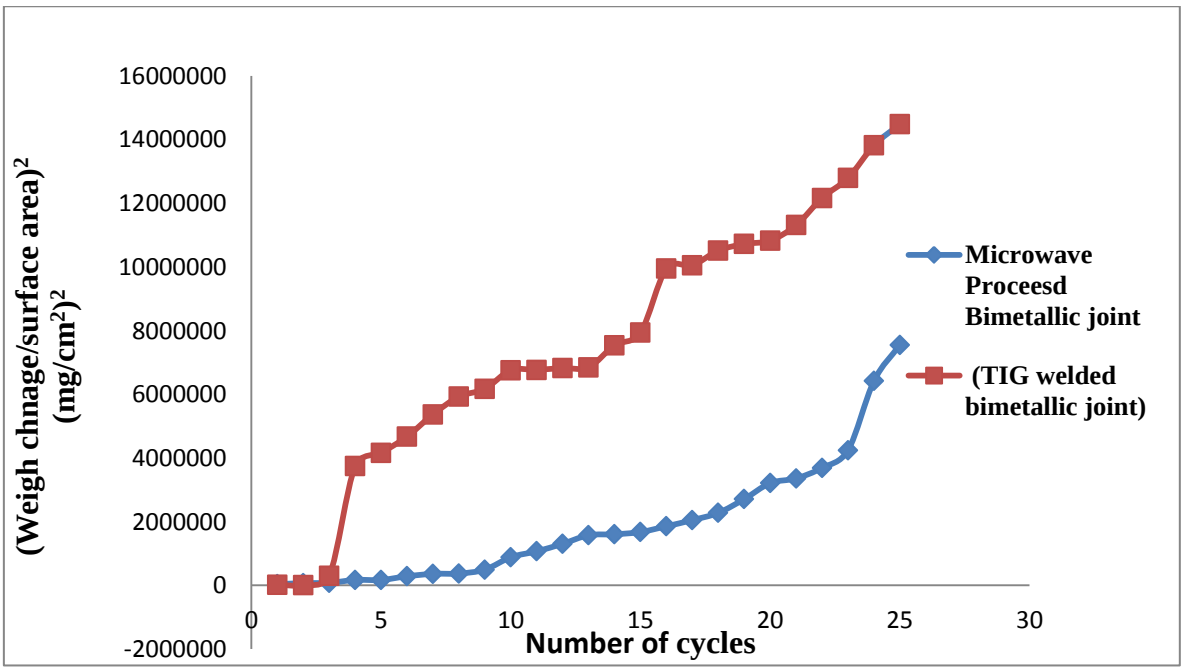

Figure 4.17 Plot of (Weight change/surface area)^2(mg/cm^2)^2 against the Number of cycles for the simulated environment of boiler for 25 cycles at 750 ℃

Table 4.3 Parabolic rate constant (K_P) for microwave processed sample and TIG welded sample after subjected to the simulated environment of boiler for 25 cycles at 750 °C

Substrates	**$K_P \times 10^{-10}$ g^2 cm^{-4} s^{-1}**
Microwave processed	67.02
TIG welded	151.68

Figure 4.17 shows the parabolic behaviour of the samples after subjected to the simulated environment of boiler for 25 cycles at 750 °C, as we can see that microwave processed sample has less K_p, means it has better corrosion resistance in the specified environment. An oxide formed has played a protective role. From the weight change plot Figure 4.16, it is clearly seen that both the samples experienced reduction in weight. This reduction in weight is related to the magnitude of spallation [66]. Weight reduction in microwave processed sample is less as compared to the TIG welded samples. From the table 4.6 it is interpreted that, less the Kp value more the corrosion resistance. So microwave processed sample has less K_p value it has higher corrosion resistance

4.3.1.3 SEM-EDS Analysis

SEM technique is used for analysing the surface morphology of the samples exposed to the environment of molten salts of 40%Na_2SO_4-40%K_2SO_4-10%NaCl-10%KCl and for the elemental analysis, EDS is done. Figure 4.18 (a-c) shows the morphology of the base metals and weld joint of microwave joined sample. From the Figure 4.18 (a) it is observed that massive porous oxide is formed along with pits on the Hastelloy C276. EDS shows the presence of high amount of chromium, nickel and oxygen. This predicts the formation of oxides of chromium or nickel. Figure 4.18 (b) shows the morphology of the weld bead of the microwave joined sample which revealed that agglomerated oxides are present and the craters are also there. In Figure 4.18 (c) shows the morphology of SS304 base metal, which clearly shows that the oxides formed are brittle in nature. EDS also confirmed by the presence of C in a large amount. This may be due to the formation of carbide in the weld zone. The weld zone of microwave welded samples is very hard due to the formation of carbides. The EDS analysis of the present study confirms the same.

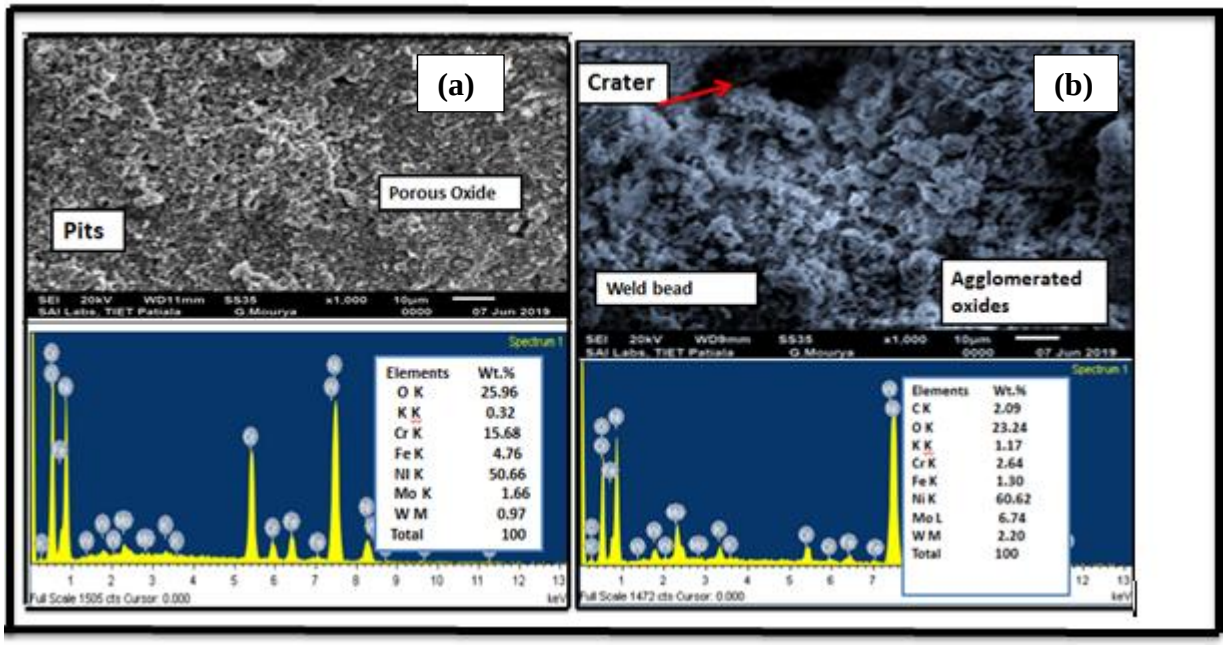

4.18 (a-b) SEM-EDS of (a) Hastelloy C276 (b) weld bead of microwave joined sample after exposure to the simulated environment of boiler for 25 cycles at 750°C.

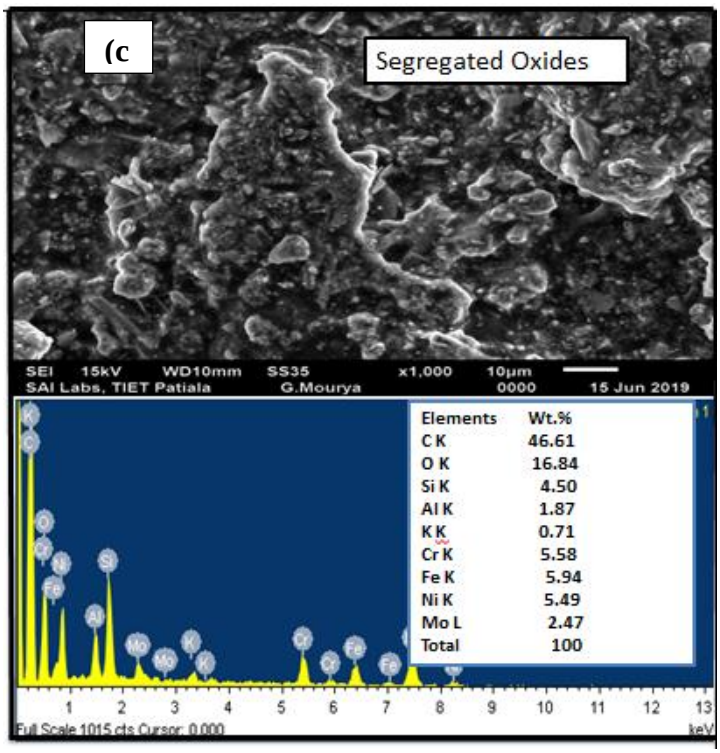

4.18 (c) SEM-EDS of SS304 of microwave joined exposure to the simulated environment of boiler for 25 cycles at 750°C.

Figure 4.19 (a-c) showing the morphology of the TIG welded sample subjected to the molten salt environment of 40%Na_2SO_4-40%K_2SO_4 -10%NaCl-10%. Figure 4.19 (a) shows the

presence of the massive oxides are formed on the surface of the Hastelloy C276 as shown in the SEM micrographs whereas in the weld bead porous and agglomerated oxides are formed as shown in Figure4.19(b). EDS confirms that the oxide so formed consist of major amount of oxygen, iron and nickel along with chromium. This depicts the formation of iron and nickel oxide in major amount. This also shows that the iron might have diffused from the SS304 towards the weld bead. From Figure 4.19 (c) it is clearly visible that porous oxides and pits are formed on the surface of SS304 consisting of iron and oxygen in major amount.

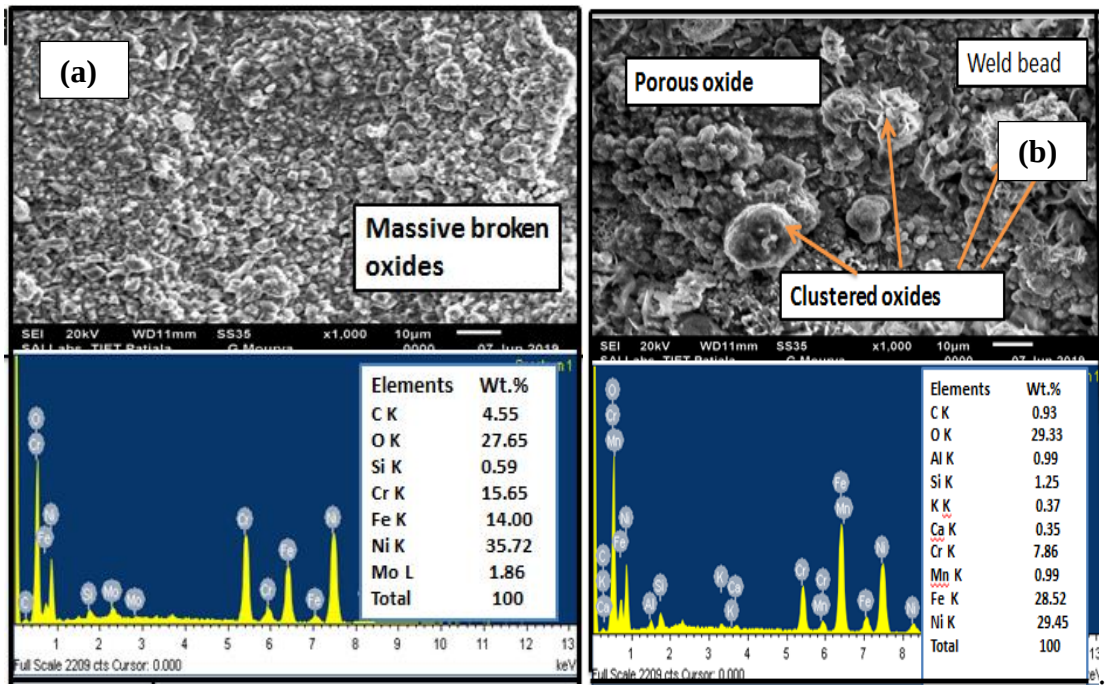

Figure 4.19 (a-b) SEM-EDS of (a) Hastelloy C276 (b) weld bead of TIG-welded sample after exposure to the molten salt environment for 25 cycles.

4.3.1.4 X-Ray Diffraction Analysis

XRD spectrum of microwave joined sample subjected to a simulated environment of boiler is shown in Figure 4.20. The major phases presents in the scale formed are Cr_2O_3, NiS_2, $NiWO_4$ MnO_2 and Ni. Peak broadening can be seen after conducting experiment. This shows the formation of amorphous phases in the weld zone. XRD analysis also confirms the formation of iron oxide in major amount as the major intense peaks of iron oxide has been formed. Presence of NiS_2 shows that nickel reacts with the sulphur present in the environment.

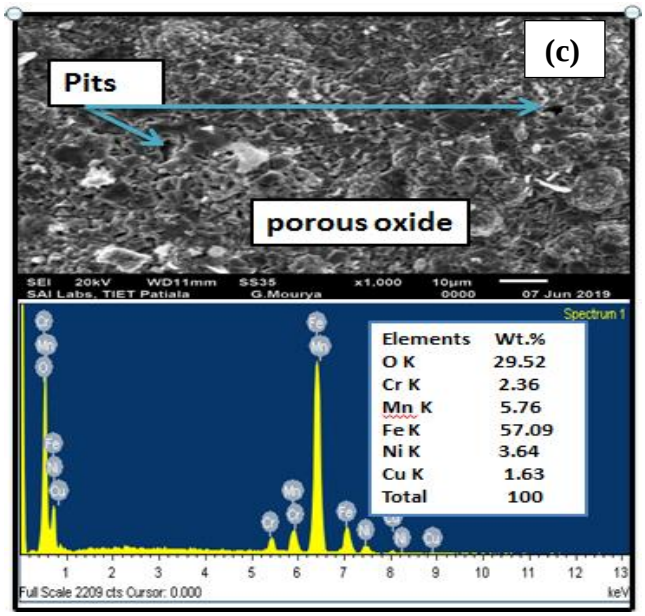

4.19 (c) SEM-EDS of SS304 of TIG-welded sample after exposure to the molten salt environment for 25 cycles.

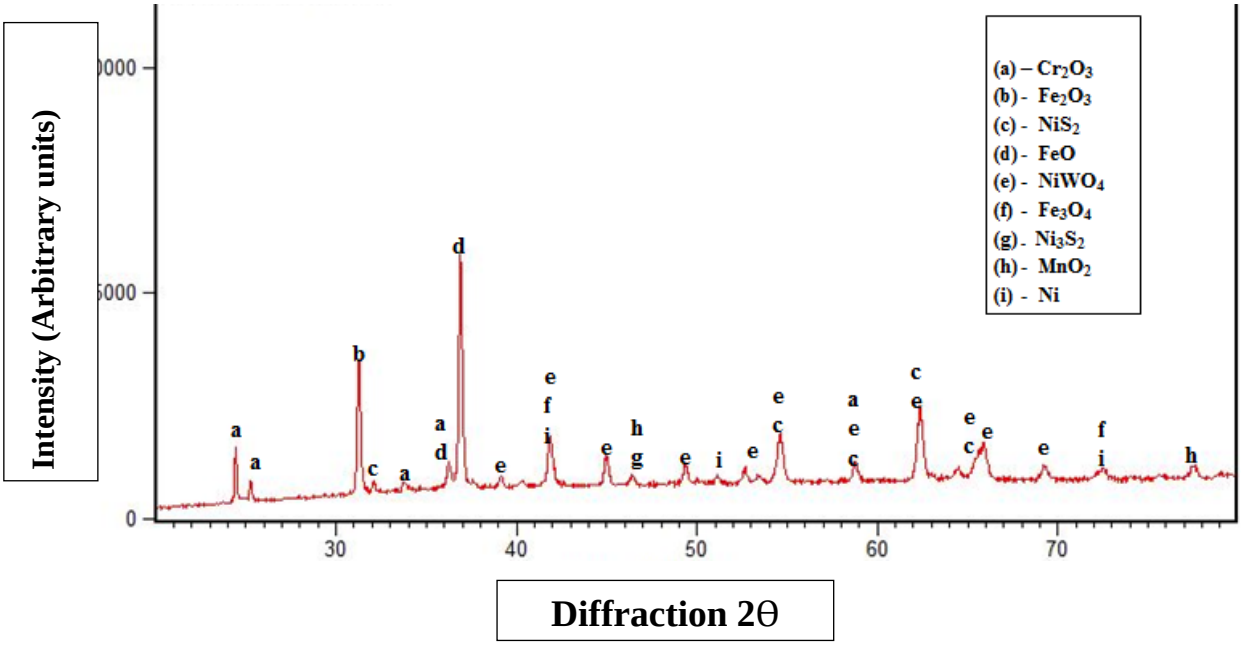

Figure 4.20 XRD spectrum of microwave joined sample subjected to simulated environment of boiler for 25 cycles at 750°C.

XRD spectrum of TIG welded sample subjected to a stimulated environment of boiler is shown in Figure 4.21. The phases presents in the scale formed are Ni_3Si_2, CrS, MnO_2, Ni_3C, Fe_3O, Fe_3C, CrO_2, Fe_2O_3, $CrCl_2$, $NaClO_2$, Ni_3C. The major phases are Ni_3Si_2, and CrS. In TIG welded zone formation of sulfides in major amount can be seen which clearly shows that the oxide so formed is not protective as sulfides have tendency to damage the oxide. Also,

chlorides were also formed in the present case. The chlorides so formed are volatile in nature. These metallic chlorides form at the interface of substrate and oxide layer and change its phase from solid to vapor. The vapor of chlorides will evaporate from the oxide leaving the oxide porous and un-protective.

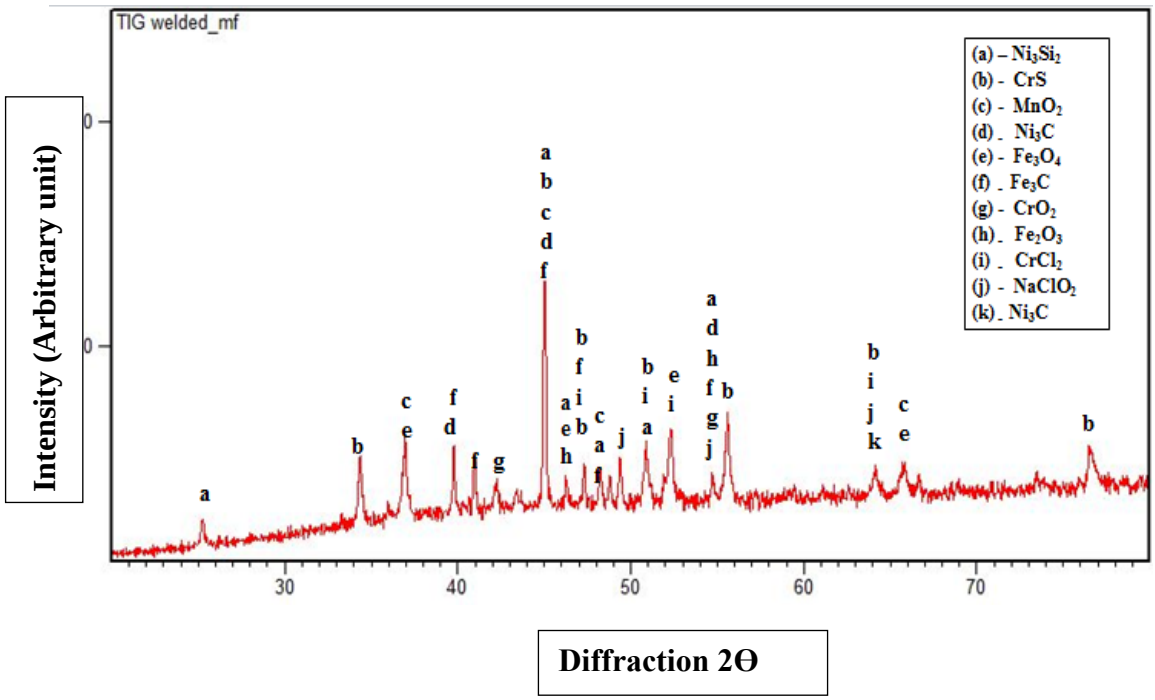

Figure 4.21 XRD spectrum of TIG-welded sample subjected to simulated environment of boiler for 25 cycles at 750° C

4.3.1.5 Elemental and X-Ray Mapping

Elemental X-ray mapping is being used for observing the presence of elements in the layer of oxide formed. Figure 4.22 shows the elemental analysis of cross-section of microwave joined sample which was subjected to the simulated environment of boiler for 25 cycles. It indicates that base metal has Ni, Fe, Cr, and Mo as the main constituent whereas the O, Fe, Ni, and Cr are in high amount in the oxide region which is confirmed by the EDS analysis as shown in Figure 4.23. Fe, Cr, Ni are responsible for the phases of NiO, Cr_2O_3, and Fe_2O_3.Whereas the elemental analysis of cross-section of scale of TIG-welded sample subjected to the molten salt environment for 25 cycles revealed that Ni, Cr, Fe, Mo are the main elements of the base metals whereas the oxide region mainly consists of O, Fe, and nickel and responsible for the formation of oxides Fe_2O_3, Cr_2O_3, and NiO. In Figure 4.22, the dense layer of chromium along with oxygen was present at the oxide substrate interface in case of microwave joined

specimens. This indicates that chromium oxide was formed at the interface which helps in providing resistance from the atmospheric corrosion. It can also notice that nickel and oxygen diffuses towards the top layer of oxide. Middle layer of the oxide scale consist of mainly iron oxide. Whereas, in case of TIG joined substrates (Figure 4.24), thin oxide layer consisting of nickel, oxygen and iron can be seen. Molybdenum was also present in the scale which shows that Mo also forms oxides.

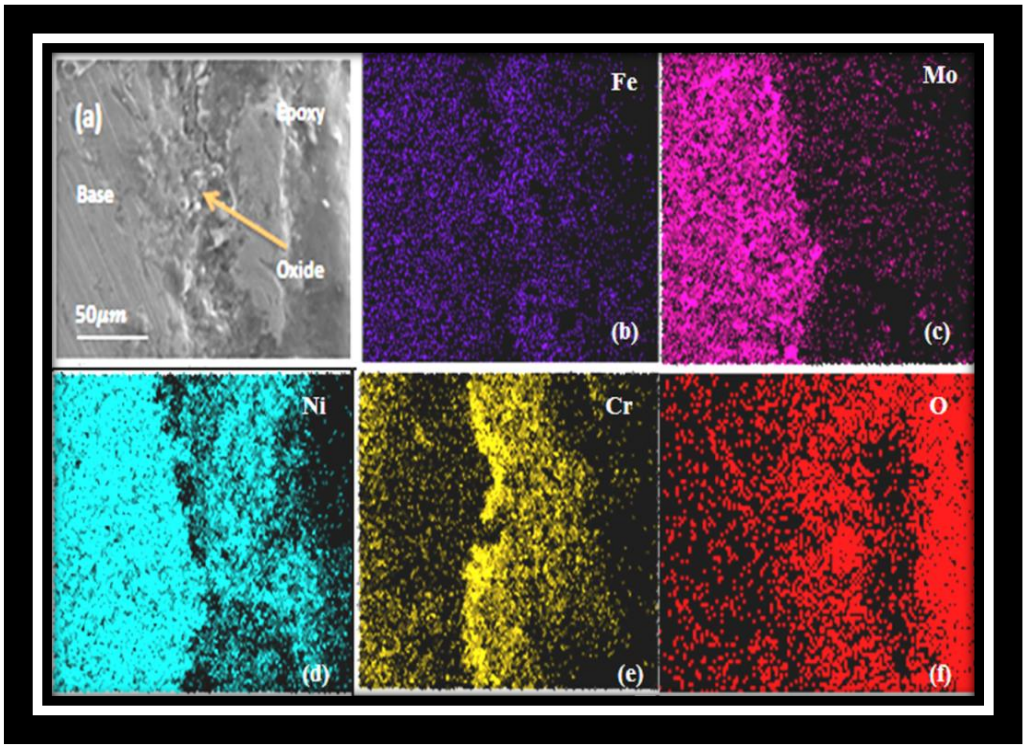

Figure 4.22 Elemental X-Ray mapping of microwave joined sample subjected to simulated environment for 25 cycles at 750° C.

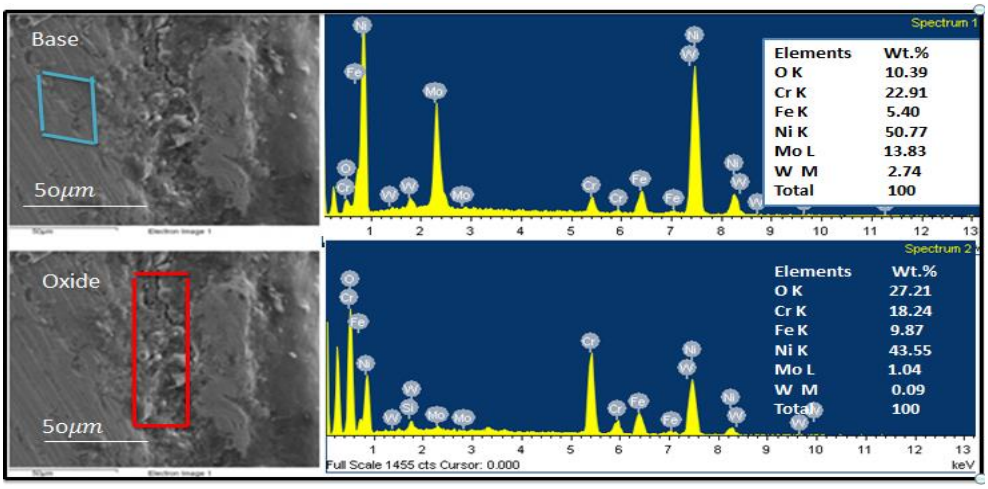

Figure 4.23 EDS of the cross-section of microwave sample subjected to simulated environment for 25 cycles at 750° C.

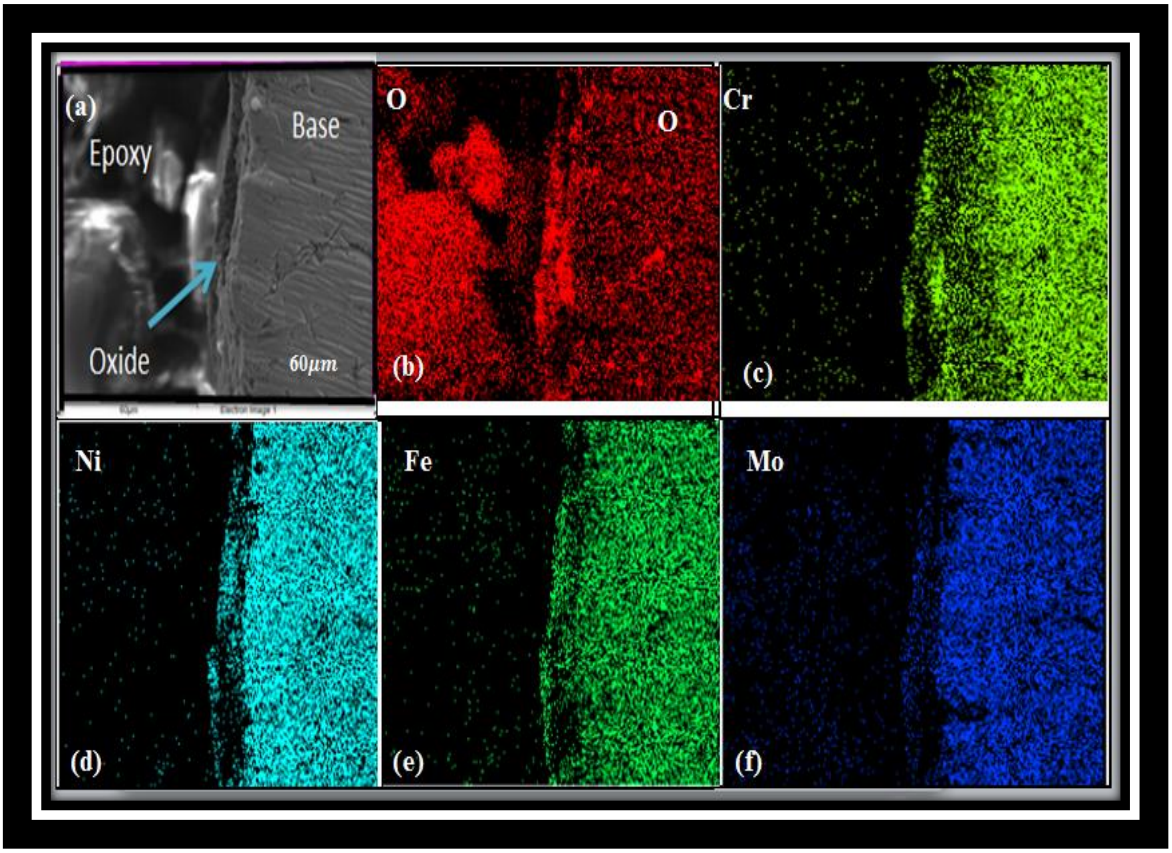

Figure 4.24 Elemental X-Ray mapping of TIG-welded sample subjected to simulated environment for 25 cycles at 750° C.

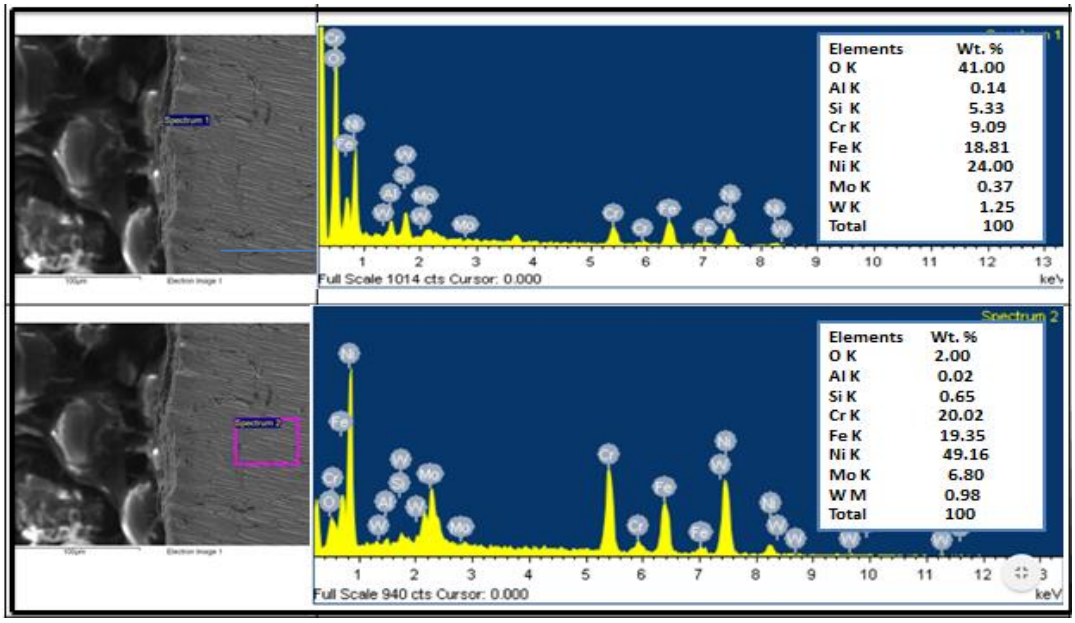

Figure 4.25 EDS of the cross-section of TIG-welded subjected to simulated Environment of boiler for 25 cycles at 750° C.

4.3.2 High-Temperature Corrosion Study in the Actual Environment of Boiler

4.3.2.1 Visual Examination

Figure 4.26shows the samples of microwave processed and TIG welded samples, after 100 h of exposure to the actual environment of the boiler. It was observed that the surface of the microwave joined sample become dark grey colour whereas the TIG welded sample is also grey with some white pits on the surface as shown in Figure 4.26. In both the specimens' red colour oxide was also seen which clearly depicts the formation of iron oxide on one side. As these welded samples, the region consisting of SS304 becomes red after exposure in high temperature area.

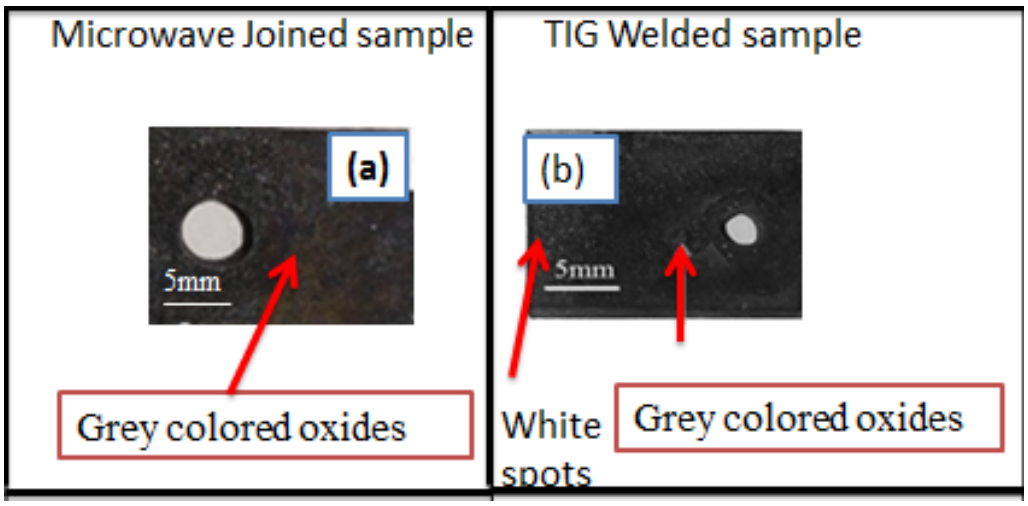

Figure 4.26 Macro photos of corroded (a) Microwave joined sample(b) TIG-welded sample after the exposure to the actual environment of boiler for 100 h

4.3.2.2 Change in Weight Measurement

Table 4.4.Change in weight of sample subjected to the boiler for 100h

Sample	Weight (before the test)	Weight (After test)
Microwave Sample	8.0513 gm.	8.0450 gm.
TIG Sample	7.0428 gm.	7.0213 gm.

4.3.2.3 SEM-EDS Analysis

For analysing the surface morphology of the samples exposed under the actual environment of a boiler, Scanning Electron Microscope is used. EDS spectrum is further used for the elemental analysis. Figure 4.27 shows the morphology of the base metals and of the joint of microwave joined sample. Figure 4.27 (a) showing the morphology of Hastelloy C276 base metal after the exposure. It is observed that massive and uneven oxides are formed, white spots are also seen which loosely bounded particles are. From Figure 4.27 (b) it is observed that oxides formed are fragile in nature and crater can also be seen in the SEM micrograph of the weld joint. Figure 4.27 (c) shows the SEM micrograph along with the EDS of the base metal SS304; it is observed that oxides fragile in nature and pits can also be seen. Figure 4.28 (a-c) shows the SEM micrograph, as well as EDS of the TIG -welded sample after exposure in the boiler for 100h.

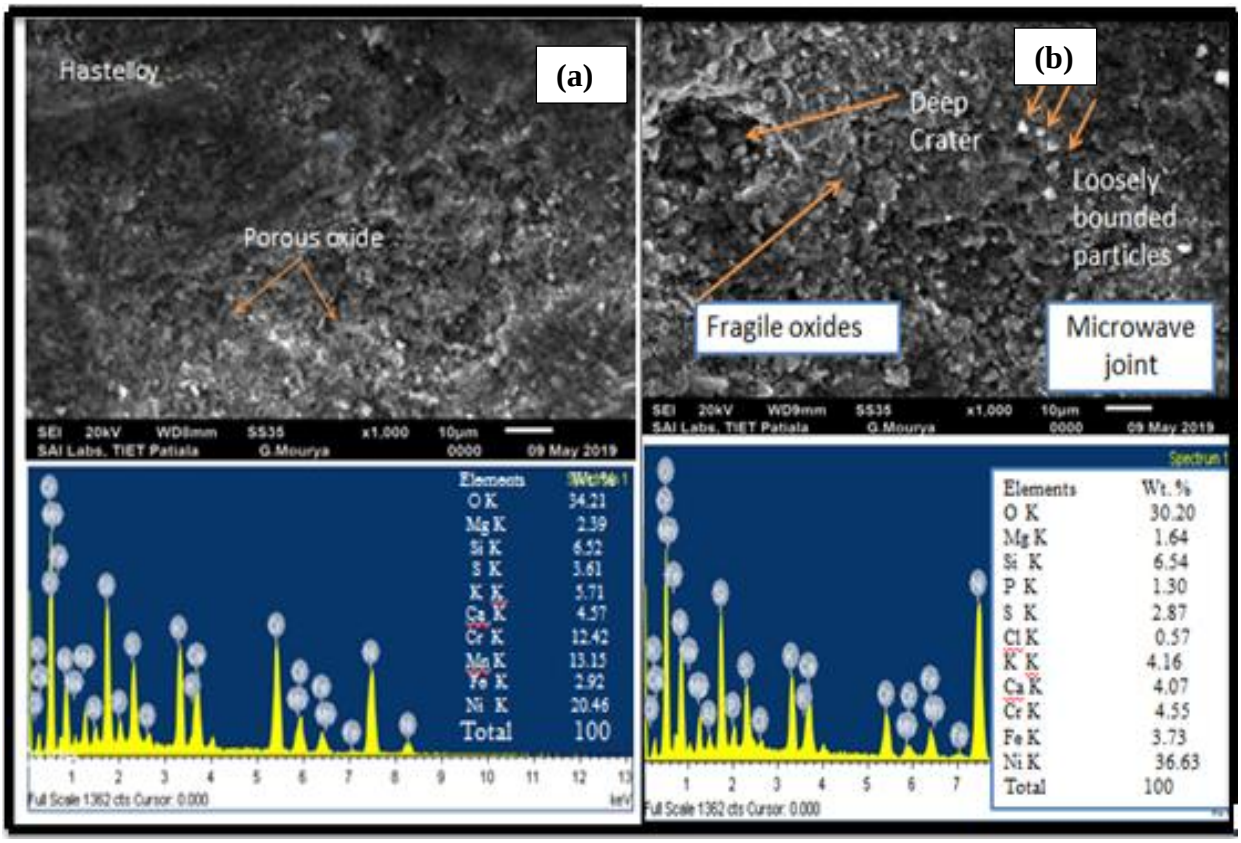

Figure 4.27SEM micrograph with EDS of (a) Hastelloy C276 (b) weld bead of microwave sample after exposure to the boiler for 100h

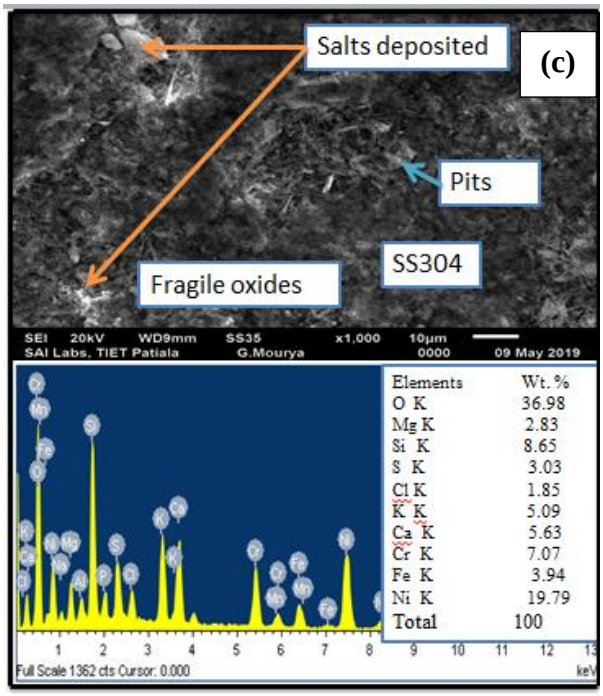

Figure 4.27 (c) SEM micrograph along with EDS of SS304 of microwave sample after exposure to the boiler for 100h

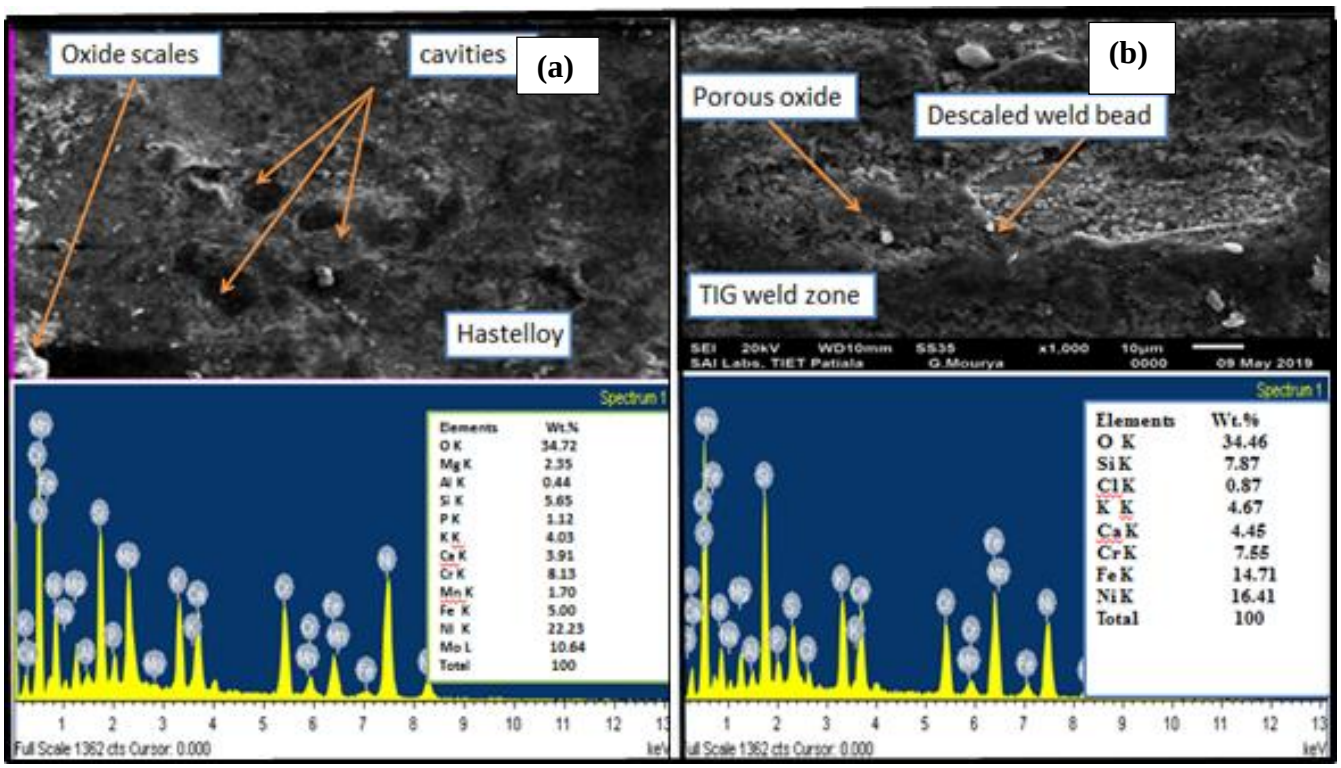

Figure 4.28 SEM-EDS of (a) Hastelloy C276 (b) weld bead of TIG WELDED sample after exposure to the boiler for 100h.

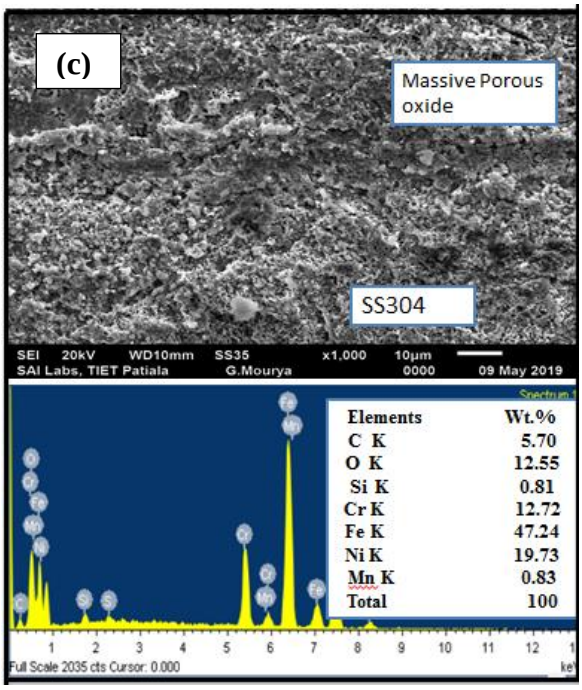

Figure 4.28 (c) SEM micrograph along with EDS of SS304 base metal of TIG welded sample after exposure to the boiler for 100h

From Figure 4.28 (a) it is observed that oxides formed on the Hastelloy C276 metal of TIG-welded are porous in nature and cavities are also present. From Figure 4.28 (b) it is observed that oxides formed on the weld zone are fragile in nature. Descaling of the weld bead is also observed along with loosely bonded particles. In Figure 4.28 (c) massive porous oxides are formed on the SS304 base metal. From EDS analysis of microwave joint. Figure 4.27 (b), it can be observed major amount of nickel and oxygen is present in the joint whereas in case of TIG welded region iron, nickel and oxygen are seen in major or amount. This clearly indicates the diffusion of iron from SS304 towards the TIG joint. This might have leads to the formation of iron oxide. It has been reported that that iron oxide is an un-protective oxide layer which can degrade the material [66].

4.3.2.4 X-Ray Diffraction Analysis

X-Ray Diffraction analysis is used for the identification of the phases present in the oxide formed on the surface of samples exposed to husk fired boiler for 100hr. XRD graph is plotted between diffraction angle 2Θ and the intensity as shown in Figure 4.29. The phase presents in the scale formed on the microwave joined sample are Cr_2O3, WO_2, $NiCl_2$, CaSiO3 Fe_2O_3, $NiCr_2O_4$ and $CrCl_2$. The major phases are Cr_2O_3, WO_2.

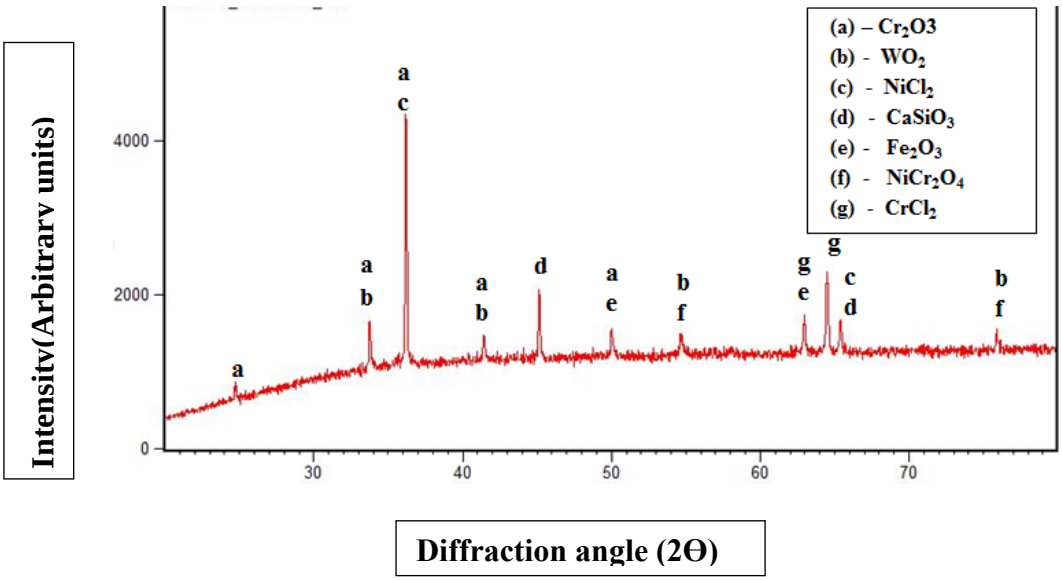

Figure 4.29 XRD spectrum of microwave joined sample subjected to the environment of boiler for 100h

Formation of major amount of chromium oxide and spinel $NiCr_2O_4$ are mainly responsible for providing protection to the substrate. From the XRD (figure 4.30) pattern of TIG welded sample ,the phases which are present are in the scale so formed are Fe_2O_3, $NiMoO_4$, $CaWO_4$, CaO, $NaCrO_2$, $CaSiO_3$, Cr_3C_2, MnO_2, Ni_3C and Ni_3Si_2.However the major phases are Fe_2O_3, $NiMoO_4$, $NaCrO_2$ and Cr_3C_2. Presence of $CaWO_4$ shows that the tungsten present in the Hastelloy C276 reacts with the calcium present in the environment to form the oxide. Formation of iron oxide is also confirmed in the XRD analysis.

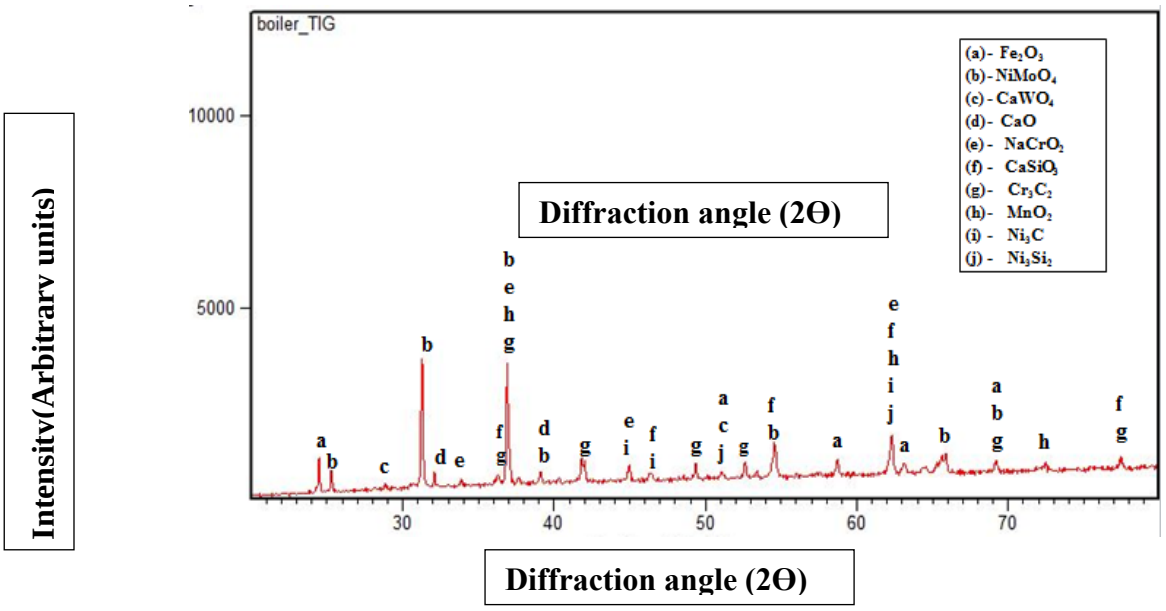

Figure 4.30 XRD spectrum of TIG-welded sample subjected to the environment of boiler for 100h

4.3.2.5 Elemental X-Ray Mapping

Elemental X-ray mapping is being used for investigating the elements present in the layer of oxide formed. The elements founded in the microwave joined sample after the exposure to the husk fired boiler at the temperature of 750 ±50 °C for 100hare Cr, Ni, Mo, Fe, O and small traces of Si and W also present as shown in Figure 4.31. From the X-Ray mapping, it is clearly visible that Cr, Ni, and Fe are present in the metal as well as in the region of oxide and Mo content is high in the metals. It is also observed that chromium depleted region exist below the oxide layer. This indicates that the chromium diffuses from the metal and forms protective oxide at the interface. The scale of oxide of microwave joined sample has Cr, O, Fe, and Ni responsible for the major phase of Fe_2O_3, Cr_2O_3.EDS analysis at base metal and oxide scale gives the exact composition of the above-mentioned elements which hereby confirms the presence of the same as shown in Figure 4.32. Both XRD and X –ray mapping results confirms the formation of chromium oxide layer on the substrate. Major amount of nickel along with oxygen is present throughout the oxide layer except at the interface. Very less amount of iron can be seen in the mapping.

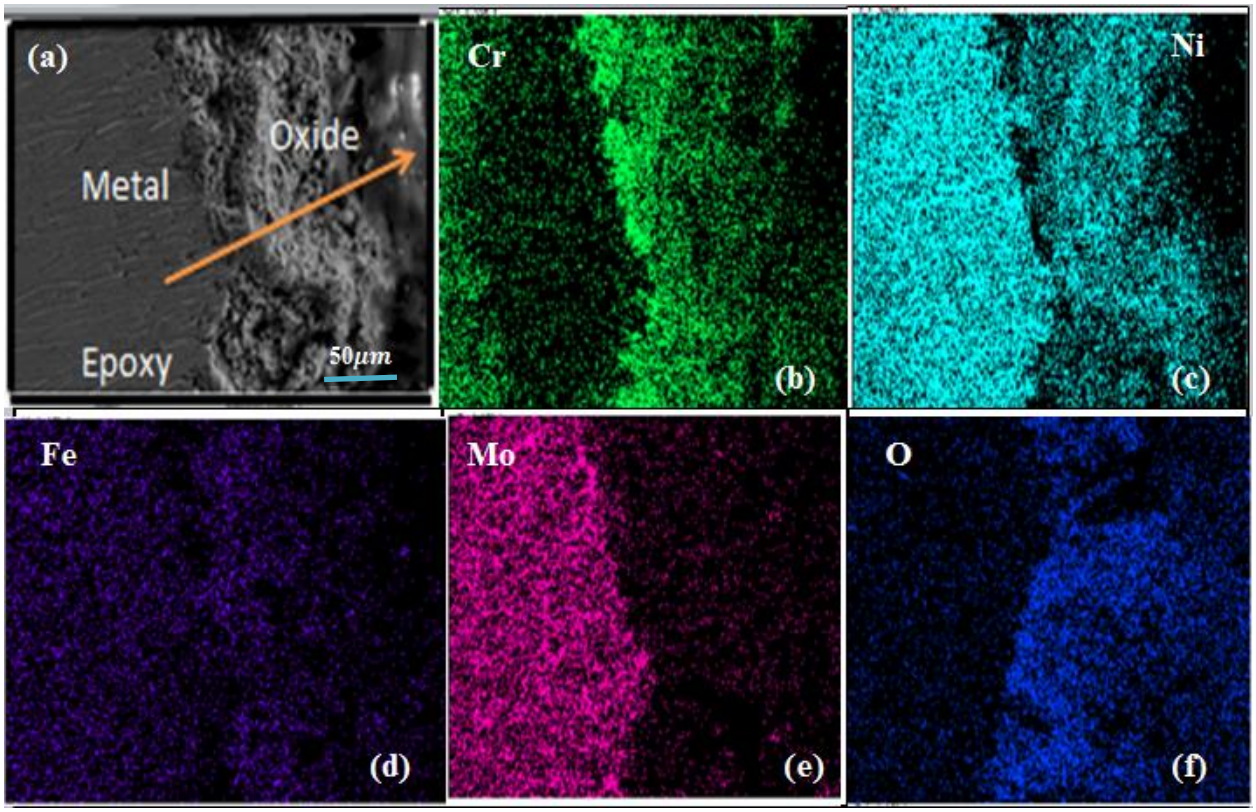

Figure 4.31 Elemental X-Ray mapping of microwave joined sample exposed in a boileratthe temperature of 750±50 °Cfor 100hr

The elements present in the TIG Welded sample exposed to husk fires boiler is shown in Figure 4.33 along with the EDS of the same in Figure 4.34 using X- ray mapping technique. It is concluded from the X-Ray elemental results that there is a high presence of Ni, Cr, Mo and Fe in the base metals and Cr, Fe, and O are present in the oxide scale and are responsible for the major phases of Cr_2O_3 and Fe_2O_3. Ni, Si, Mo, and W are present in the small trace which is responsible for the phases of $(Cr, Fe)_2O_3$. Composition of the above-mentioned elements is shown in Figure 4.34.in EDS analysis.

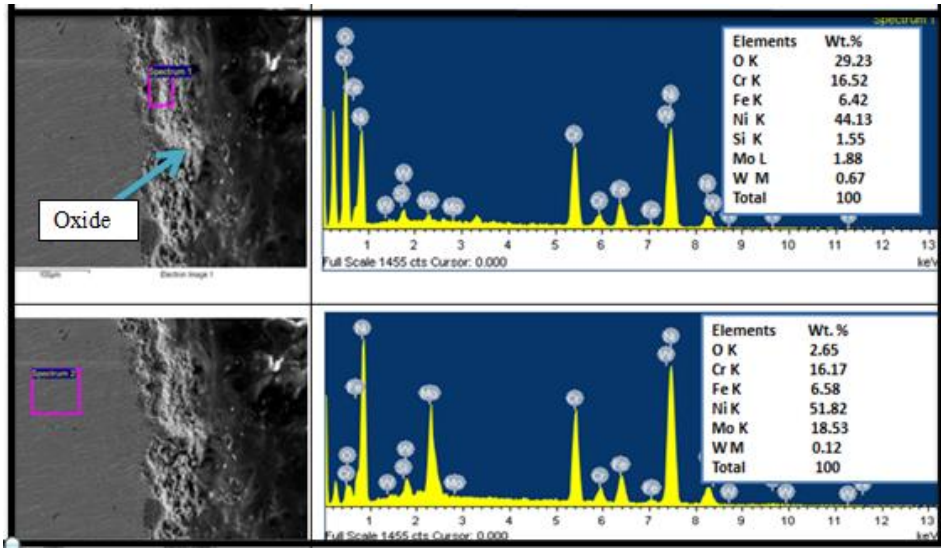

Figure 4.32 EDS of the cross-section of microwave joined sample exposed to the boiler at temperature 750 ± 50° C for 100h

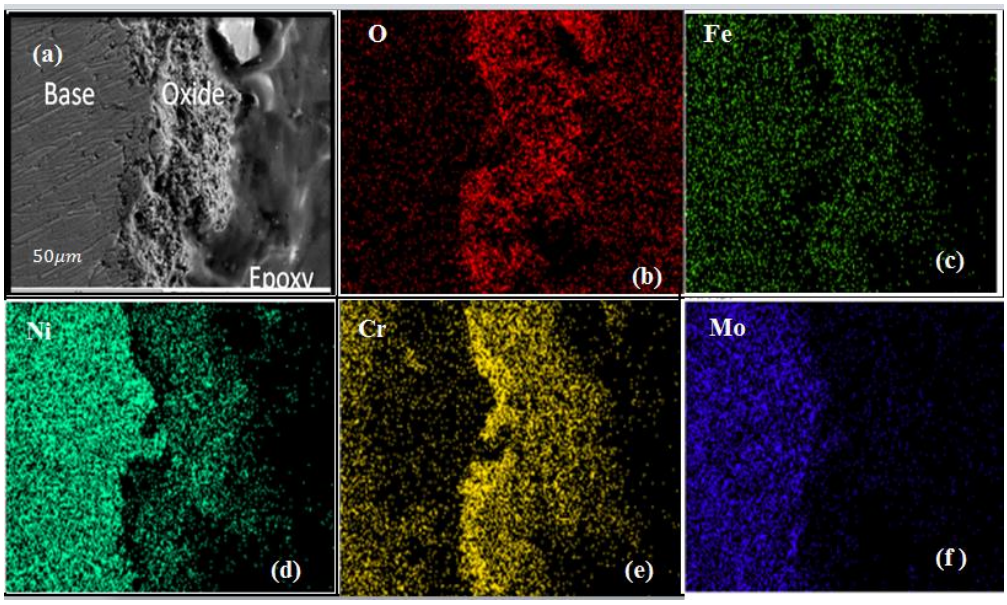

Figure.4.33 Elemental X-Ray mapping of TIG-welded sample exposed in a boilerat the temperature of 750 ±50 °C for 100hr.

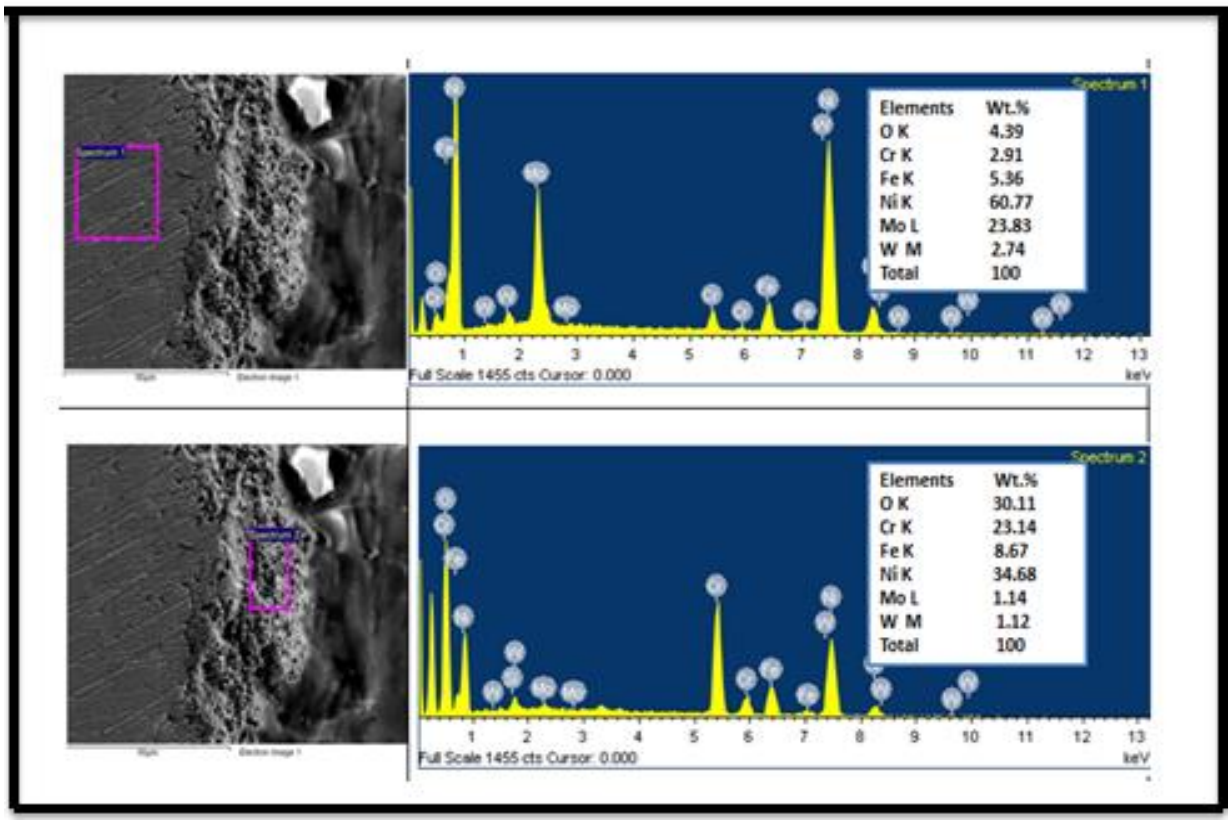

Figure 4.34 EDS of the cross-section of TIG-welded sample exposed to the boiler at temperature 750 ± 50° C for 100h

4.4 Measurement of thickness loss

Rate of corrosion of the sample can be calculated by thickness loss or the mass loss of the sample in the given environment. The formula for the calculation of the same is given below. A most common unit for corrosion rate is mpy that is milli-inches per year.

$$Corrosion\ Rate, mpy = \frac{Thickness\ loss, micron}{25.4} = \frac{(mass\ loss, g) \times 3450000}{8760 \times SA \times d}$$

Where d is density (g/cm$^{3)}$ and SA is surface area (cm^2)

In other way mpy can be calculated as follows: one year has 8730 hrs and 1mm is 39.37 mills. So for thickness loss of "z" for 1000 hrs., mpy is (z) × 39.37 × $(\frac{8760}{1000})$

Thickness loss in the microwave joined sample is 0.21mm and in case of TIG-welded sample is 0.35mm, when the samples subjected to the actual environment of the boiler at 750 ± 50°C for 100h.

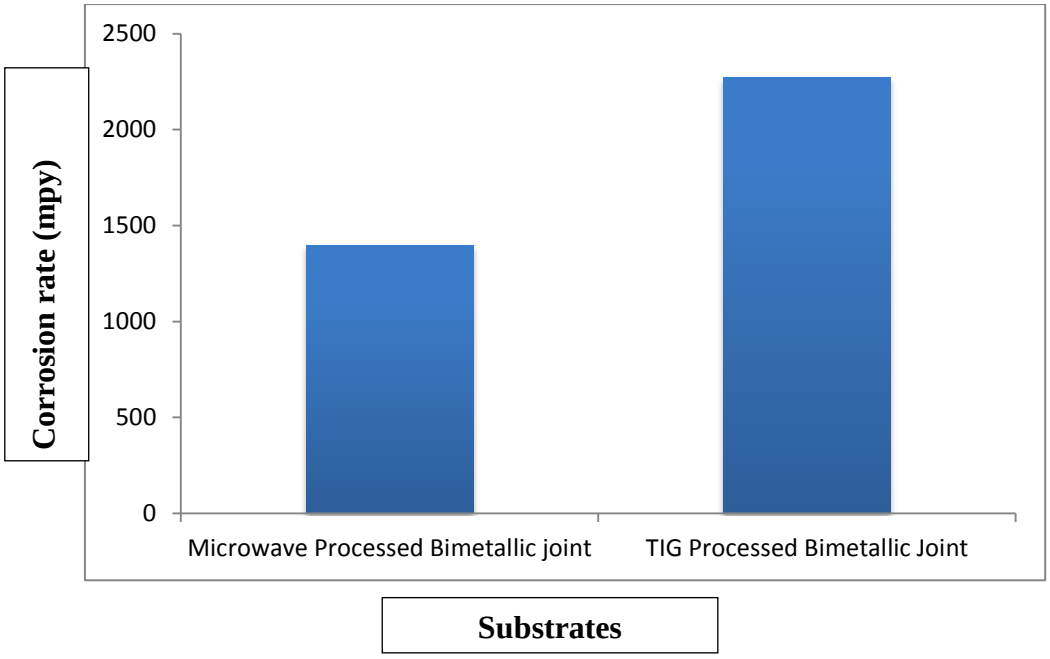

Figure 4.35 Measurement of thickness loss of Microwave processed bimetallic joint and TIG processed bimetallic joint after subjected to the boiler at 750 ±50 °C for 100h.

Chapter 5

Conclusions and Future Scope

5.1 Microstructural and Mechanical Characterizations

- Microwave joint has been successfully developed for the materials (Hastelloy C276 and SS304) using the nickel powder in time of 8 min.
- Micro hardness tests were conducted across the weld joint and the interface results clearly show that the hardness value at the joint is higher in case of microwave joined sample as compared to the TIG welded sample because of the presence of carbides whereas the hardness at the interface is more in case of TIG-welded sample.
- Tensile strength of the microwave joined sample is more than a TIG-welded sample because of better metallurgical property and fewer defects in the microwave processed sample as compared to the TIG welded sample.

5.2 Hot Corrosion in Simulated Environment of Boiler for 25 cycles at 750°C

- Based on the change in weight, a graph has plotted for 25 cycles, in a simulated environment of boiler (60% Na_2SO_4-60% K_2SO_4-10% NaCl-10% KCl) at 750°C. Weight loss is recorded in both samples however weight loss is more in the case of TIG-welded sample.
- The visual analysis which has been done just after each cycle shows the formation of oxides. In the case of microwave joined sample, greenish oxide in the form of powder along with spallation was seen and in TIG welded samples oxides are of dark grey colour along with the spallation was seen.
- SEM analysis depicts the formation of fragile oxides along with clustered oxides in case of both weld joints. EDS analysis shows the presence of C, W, Mo, Fe in a major amount which might have deposited on the surface of the substrate that causes the more degradation of the samples.
- In case of microwave processed joints, XRD analysis showed the intense peaks of Cr_2O_3 and Fe_2O_3 whereas in case of TIG welded joints major peaks of Ni_3S_2, and Fe_2O_3 indicated. This Cleary showed the occurrence of sulphidation in case of TIG welding.

.

5.3 Hot Corrosion in Actual Environment of Boiler

- The visual analysis which has been done just after the 100h, clearly show the formation of the dark grey oxide layer on the surface of both TIG and Microwave processed samples. However, no spallation or sputtering was seen on both the substrates.
- A weight change measurement clearly depicts the minor loss in weight after 100h of exposure.
- SEM-EDS depict the formation of fragile oxides in case of both weld joints. EDS analysis shows the presence of Ca, K, S, Si, Mg in a major amount which might have deposited on the surface of the substrates from the boiler environment.
- XRD analysis confirms the presence of calcium in the form of CaO on the surface of both samples. XRD also revealed the formation of Cr_2O_3, WO_2 and $NiCl_2$ in case of corroded microwave processed joints. Whereas in case of corroded TIG welded joints major peaks of Fe_2O_3 and $NiMoO_4$ were observed.
- X- Ray mapping shows the presence of Cr, Fe, Ni, and O in major proportion in oxides scale. Chromium depleted zone was observed below the oxide region due to the diffusion of chromium from substrate towards the oxide. Chromium oxides so formed provides protection from the corrosive atmosphere by inhibiting the diffusion of corrosive species in the metal.

5.4 Future Scope

1. To evaluate the performance of microwave joined AISI 304 and Monel 400 under Na_2SO_4-NaCl at 800°C.
2. To study the mechanical and corrosive properties of microwave welded duplex stainless steel 2205 and austenitic stainless steel 304.
3. To study the microstructural, mechanical and corrosion performance of microwave welded AISI 304 and AISI 347
4. To compare the hot corrosion performance of dissimilar weldments welded by TIG and microwave under various extreme environment.

References

1. Otero, E., Pardo, A., Hernaez, J., & Perez, F. J. (1991). The hot corrosion of IN-657 superalloy in Na2SO4-V2O5 melt eutectic. *Corrosion science*, *32*(7), 677-683.
2. Lai, G. Y. (1990). High temperature corrosion of engineering alloys.
3. Zheng, L., Maicang, Z., & Jianxin, D. (2011). Hot corrosion behavior of powder metallurgy Rene95 nickel-based superalloy in molten NaCl–NaSO4 salts. *Materials & Design*, *32*(4), 1981-1989.
4. Raman, R. S., & Muddle, B. C. (2002). High temperature oxidation in the context of life assessment and microstructural degradation of weldments of 2.25 Cr–1Mo steel. *International Journal of Pressure Vessels and Piping*, *79*(8-10), 585-590.
5. Ramkumar, K. D., Arivazhagan, N., & Narayanan, S. (2012). Effect of filler materials on the performance of gas tungsten arc welded AISI 304 and Monel 400. *Materials & Design*, *40*, 70-79.
6. Wang, S., Ma, Q., & Li, Y. (2011). Characterization of microstructure, mechanical properties and corrosion resistance of dissimilar welded joint between 2205 duplex stainless steel and 16MnR. *Materials & Design*, *32*(2), 831-837.
7. Adamiec, J. (2011). Hot cracking of welded joints of the 7CrMoVTiB 10-10 (T/P24) steel. In *IOP Conference Series: Materials Science and Engineering* (Vol. 22, No. 1, p. 012001). IOP Publishing.
8. Reddy, G. M., & Rao, K. S. (2009). Microstructure and mechanical properties of similar and dissimilar stainless steel electron beam and friction welds. *The International Journal of Advanced Manufacturing Technology*, *45*(9-10), 875.
9. Arivazhagan, N., Ramkumar, K. D., Karthikeyan, S., Manikandan, M., Narayanan, S., & Surendra, S. (2012, November). A Comparative Study of Oxidation and Hot Corrosion of Electron Beam Welded Low Alloy Steel and Stainless Steel in Different Corrosive Environments. In *International Conference on Intelligent Robotics, Automation, and Manufacturing* (pp. 442-449).
10. Arivazhagan, N., Singh, S., Prakash, S., & Reddy, G. M. (2009). Hot corrosion studies on dissimilar friction welded low alloy steel and austenitic stainless steel under chlorine containing salt deposits under cyclic conditions. *Corrosion engineering, Science and technology*, *44*(5), 369-380\
11. Ramkumar, K. D., Arivazhagan, N., & Narayanan, S. (2012). Effect of filler materials on the performance of gas tungsten arc welded AISI 304 and Monel 400. *Materials & Design*, *40*, 70-79.

12. Wang, W., Wang, X., Zhong, W., Hu, L., & Hu, P. (2014). Failure analysis of dissimilar steel welded joints in a 3033t/h USC boiler. *Procedia materials science*, *3*, 1706-1710.
13. Thong-On, A., & Boonruang, C. (2016). Design of boiler welding for improvement of lifetime and cost control. *Materials*, *9*(11), 891..
14. Khidhir, G. I., & Baban, S. A. (2019). Efficiency of dissimilar friction welded 1045 medium carbon steel and 316L austenitic stainless steel joints. *Journal of Materials Research and Technology*, *8*(2), 1926-1932.
15. Chhibber, R., Arora, N., Gupta, S. R., & Dutta, B. K. (2006). Use of bimetallic welds in nuclear reactors: associated problems and structural integrity assessment issues. *Proceedings of the Institution of Mechanical Engineers, Part C: Journal of Mechanical Engineering Science*, *220*(8), 1121-1133.
16. Lancaster, J. F. (1973). Failures of boilers and pressure vessels: their causes and prevention. *International Journal of Pressure Vessels and Piping*, *1*(2), 155-170.
17. Lai, G. Y., & Hulsizer, P. N. (2000, January). Corrosion and Erosion/Corrosion Protection by Modern Weld Overlays in Low NOx, Coal-Fired Boilers. In *CORROSION 2000*. NACE International.
18. Korkmaz, E., Gülsöz, A., & Meran, C. (2019). The Friction Weldability of AA6063 Tube to AA6082 Tube Plates Using an External Tool. In *Materials Design and Applications II* (pp. 427-437). Springer, Cham.
19. Ribic, B., Palmer, T. A., & DebRoy, T. (2009). Problems and issues in laser-arc hybrid welding. *International Materials Reviews*, *54*(4), 223-244.
20. Badiger, R. I., Narendranath, S., & Srinath, M. S. (2015). Joining of Inconel-625 alloy through microwave hybrid heating and its characterization. *Journal of Manufacturing Processes*, *18*, 117-123..
21. Bansal, A., Sharma, A. K., Kumar, P., & Das, S. (2012). Application of electromagnetic energy for joining of Inconel 718 plates. *imanager's Journal of Mechanical Engineering*, *2*(4), 18-23.
22. Sharma, A. K., & Gupta, D. (2012). On microstructure and flexural strength of metal–ceramic composite cladding developed through microwave heating. *Applied Surface Science*, *258*(15), 5583-5592.
23. Keyson, D., Volanti, D. P., Cavalcante, L. S., Simoes, A. Z., Souza, I. A., Vasconcelos, J. S., ... & Longo, E. (2007). Domestic microwave oven adapted for fast

heat treatment of Ba0. 5Sr0. 5 (Ti0. 8Sn0. 2) O3 powders. *Journal of Materials Processing Technology*, *189*(1-3), 316-319.

24. Ku, H.S.; Stores, E.; Ball, J.A.R. Review—microwave processing of materials: PartI. The Honking Institution of Engineers Transactions 2001, 8, 31–37.
25. Lauf, R. J., Bible, D. W., Johnson, A. C., & Everleigh, C. A. (1993). Two to 18 GHz broadband microwave heating systems. *Microwave Journal*, *36*(11), 24-30.
26. Thostenson, E. T., & Chou, T. W. (1999). Microwave processing: fundamentals and applications. *Composites Part A: Applied Science and Manufacturing*, *30*(9), 1055-1071.
27. Spencer, P. L. Method of treating foodstuffs. US Patient 2495429 A, 1950.
28. Menéndez, J. A., Arenillas, A., Fidalgo, B., Fernández, Y., Zubizarreta, L., Calvo, E. G., & Bermúdez, J. M. (2010). Microwave heating processes involving carbon materials. *Fuel Processing Technology*, *91*(1), 1-8.
29. Bajpai, P. K., Singh, I., & Madaan, J. (2012). Joining of natural fiber reinforced composites using microwave energy: Experimental and finite element study. *Materials & Design*, *35*, 596-602.
30. Zhou, J., Shi, C., Mei, B., Yuan, R., & Fu, Z. (2003). Research on the technology and the mechanical properties of the microwave processing of polymer. *Journal of Materials Processing Technology*, *137*(1-3), 156-158.
31. Agrawal, D. (2010). Latest global developments in microwave materials processing. *Materials Research Innovations*, *14*(1), 3-8.
32. Bruce, R. W., Fliflet, A. W., Huey, H. E., Stephenson, C., & Imam, M. A. (2010). Microwave sintering and melting of titanium powder for low-cost processing. In *Key Engineering Materials* (Vol. 436, pp. 131-140). Trans Tech Publications.\
33. Giberson, R. T., & Sanders, M. (2009). The real benefits of microwave-assisted processing go beyond time savings. *Microscopy and Microanalysis*, *15*(S2), 926-927.
34. Wang, J., Binner, J., Pang, Y., & Vaidhyanathan, B. (2008). Microwave-enhanced densification of sol–gel alumina films. *Thin solid films*, *516*(18), 5996-6001.

35. Fang, Y., Cheng, J., Roy, R., Roy, D. M., & Agrawal, D. K. (1997). Enhancing densification of zirconia-containing ceramic-matrix composites by microwave processing. *Journal of materials science*, *32*(18), 4925-4930.

36. Wong, W. L. E., & Gupta, M. (2007). Improving overall mechanical performance of magnesium using nano-alumina reinforcement and energy efficient microwave assisted processing route. *Advanced Engineering Materials*, *9*(10), 902-909.

37. Singh, S., Gupta, D., Jain, V., & Sharma, A. K. (2015). Microwave processing of materials and applications in manufacturing industries: a review. *Materials and Manufacturing Processes*, *30*(1), 1-29.

38. Roy, R., Agrawal, D., Cheng, J., & Gedevanishvili, S. (1999). Full sintering of powdered-metal bodies in a microwave field. *Nature*, *399*(6737), 668.

39. Sharma, A. K., Srinath, M. S., & Kumar, P. (1994). Microwave joining of metallic materials. *Indian Patent application no*.

40. Upadhyaya, A., Tiwari, S. K., & Mishra, P. (2007). Microwave sintering of W–Ni–Fe alloy. *Scripta Materialia*, *56*(1), 5-8.

41. Mondal, A., Upadhyaya, A., & Agrawal, D. (2013). Effect of heating mode and copper content on the densification of W-Cu alloys. *Indian Journal of Materials Science*, *2013*.

42. Siores, E., & Do Rego, D. (1995). Microwave applications in materials joining. *Journal of Materials Processing Technology*, *48*(1-4), 619-625.

43. Olivas-Ogaz, M. A., Eklund, J., Persdotter, A., Sattari, M., Liske, J., Svensson, J. E., & Jonsson, T. (2019). The Influence of Oxide-Scale Microstructure on KCl (s)-Induced Corrosion of Low-Alloyed Steel at 400° C. *Oxidation of Metals*, *91*(3-4), 291-310.

44. Okoro, S. C., Montgomery, M., Frandsen, F. J., & Pantleon, K. (2018). Influence of Preoxidation on High-Temperature Corrosion of a FeCrAl Alloy Under Conditions Relevant to Biomass Firing. *Oxidation of Metals*, *89*(1-2), 99-122.

45. Li, P., Li, T. J., Zhao, J., & Pang, S. J. (2018). Hot corrosion behaviors of Super

304H austenitic stainless steel pre-coated in Na 2 SO 4–25% NaCl mixture salt film. *Journal of Iron and Steel Research International*, *25*(11), 1149-1155.

46. Reddy, L., Sattari, M., Davis, C. J., Shipway, P. H., Halvarsson, M., & Hussain, T. (2019). Influence of KCl and HCl on a Laser Clad FeCrAl Alloy: In-Situ SEM and Controlled Environment High Temperature Corrosion. *Corrosion Science*.

47. Arivazhagan, N., Singh, S., Prakash, S., & Reddy, G. M. (2011). Investigation on AISI 304 austenitic stainless steel to AISI 4140 low alloy steel dissimilar joints by gas tungsten arc, electron beam and friction welding. *Materials & Design*, *32*(5), 3036-3050.

48. Hosseini, H. S., Shamanian, M., & Kermanpur, A. (2016). Microstructural and weldability analysis of Inconel617/AISI 310 stainless steel dissimilar welds. *International Journal of Pressure Vessels and Piping*, *144*, 18-24.

49. Hajiannia, I., Shamanian, M., & Kasiri, M. (2013). Microstructure and mechanical properties of AISI 347 stainless steel/A335 low alloy steel dissimilar joint produced by gas tungsten arc welding. *Materials & design*, *50*, 566-573.

50. Ramkumar, K.D., Arivazghan, N., & Nrayanan, S.(2012). Effect of filler materials on the performances of gas tungsten arc welded AISI 304 and Monel 400. Material & Design, 40,70-79.

51. Gupta, D.; Sharma, A.K. (2014). Microwave cladding: a new approach in surface engineering. Journal of Manufacturing Processes, 16, 176–182.

52. Bansal, A., Sharma, A. K., Kumar, P., & Das, S. (2014). Characterization of bulk stainless steel joints developed through microwave hybrid heating. *Materials Characterization*, *91*, 34-41.

53. Gupta, P., & Kumar, S. (2014). Investigation of stainless steel joint fabricated through microwave energy. *Materials and Manufacturing Processes*, *29*(8), 910-915.

54. Ramkumar, K. D., Abraham, W. S., Viyash, V., Arivazhagan, N., & Rabel, A. M. (2017). Investigations on the microstructure, tensile strength and high temperature corrosion behaviour of Inconel 625 and Inconel 718 dissimilar joints. *Journal of Manufacturing Processes*, *25*, 306-322.

55. Montgomery, M., Malede, Y. C., Wu, D., & Dahl, K. V. (2018). Danish Experiences in Biomass Corrosion and Recent Areas of Research. *Corrosion*, *75*(4), 358-366.

56. Hashim, A. A., Hammood, A. S., & Hammadi, N. J. (2015). Evaluation of High-Temperature Oxidation Behavior of Inconel 600 and Hastelloy C-22. *Arabian Journal for Science and Engineering*, *40*(9), 2739-2746.

57. Mortezaie, A., & Shamanian, M. (2014). An assessment of microstructure, mechanical properties and corrosion resistance of dissimilar welds between Inconel 718 and 310S austenitic stainless steel. *International Journal of Pressure Vessels and Piping*, *116*, 37-46.

58. Naffakh, H., Shamanian, M., & Ashrafizadeh, F. (2009). Dissimilar welding of AISI 310 austenitic stainless steel to nickel-based alloy Inconel 657. *Journal of materials processing technology*, *209*(7), 3628-3639.

59. Wang, J., Lu, M. X., Zhang, L., Chang, W., Xu, L. N., & Hu, L. H. (2012). Effect of welding process on the microstructure and properties of dissimilar weld joints between low alloy steel and duplex stainless steel. *International Journal of Minerals, Metallurgy, and Materials*, *19*(6), 518-524.

60. Wu, W., Hu, S., & Shen, J. (2015). Microstructure, mechanical properties and corrosion behavior of laser welded dissimilar joints between ferritic stainless steel and carbon steel. *Materials & Design (1980-2015)*, *65*, 855-861.

61. Mittal, R., & Sidhu, B. S. (2018). Oxidation behaviour of T91/347H welds. *Journal of Materials Processing Technology*, *261*, 266-279.

62. Mittal, R., & Sidhu, B. S. (2015). Microstructures and mechanical properties of dissimilar T91/347H steel weldments. *Journal of Materials Processing Technology*, *220*, 76-86.

63. Ramkumar, K. D., Arivazhagan, N., Narayanan, S., & Mishra, D. (2014). Hot corrosion behavior of monel 400 and AISI 304 dissimilar weldments exposed in the molten salt environment containing Na2SO4+ 60% V2O5 at 600° C. *Materials Research*, *17*(5), 1273-1284.

64. Sharma, A. K., & Gupta, D. (2012). On microstructure and flexural strength of metal–ceramic composite cladding developed through microwave heating. *Applied Surface Science*, *258*(15), 5583-5592.

65. Srinath, M. S., Sharma, A. K., & Kumar, P. (2011). Investigation on microstructural and mechanical properties of microwave processed dissimilar joints. *Journal of manufacturing processes*, *13*(2), 141-146.

66. Kamal, S., Kumar, C. V., & Abdul-Rani, A. M. (2014). Hot Corrosion Studies in Coal Fired Boiler Environment. In *MATEC Web of Conferences* (Vol. 13, p. 03005). EDP Sciences.